

# STANDARD HIGGS BOSON SEARCHES AT LEP 2

Giampiero PASSARINO<sup>ab</sup>,

<sup>a</sup> Dipartimento di Fisica Teorica, Università di Torino, Torino, Italy

<sup>b</sup> INFN, Sezione di Torino, Torino, Italy

The process  $e^+e^- \rightarrow \bar{b}b\bar{f}f$  with  $f = \nu$ , or  $f =$  charged lepton or  $f = u, d$  quark is analyzed in the range of LEP 2 energies. In the near future LEP 2 will represent a unique opportunity for a direct search of a Higgs boson of mass  $> 65$  GeV. The whole emphasis has been put on a self consistent study of the standard Higgs boson properties. Indeed there is the actual possibility of testing a calculation which uses the full matrix elements for  $e^+e^-$  annihilation into 4-fermions with the experimental data, beyond the usual approximation of computing production cross section  $\times$  branching ratios of Higgs into decay products. Of course, given the fact that the number of collected events at LEP 2 will be limited and because of the low statistics one could proceed with a different strategy: for discovery physics elaborated tools are unnecessary. However the precise theoretical calculation is at our disposal already now, thanks to the combined effort of several groups, and it is extremely interesting and appealing to apply the corresponding machinery to an analysis – as complete as possible – of standard Higgs boson physics. Calculation of the total cross sections and of different kinds of differential distributions at the partonic level are made available to access the widest information for choosing cuts, for discussing the physics of a standard Higgs boson with a mass around 90 GeV where the Higgs and the  $Z$  signal become degenerate and for a comprehensive analysis of the various background components.

*PACS Classification:* 11.15.-q, 12.15.Ji, 12.20.Fv, 14.70.Fm

*Keywords:* LEP 2 physics, Standard model four-fermion production, Standard Higgs Boson searches, Total and differential cross sections, Exact matrix elements, QCD perturbative corrections.

Submitted to Nucl. Phys. B

# 1 Introduction

With the new experimental data from the LEP Collaborations and the increasing achieved experimental accuracy there is an indirect evidence for a Higgs boson with a mass approximately below 500 GeV in the minimal standard model of the unified electroweak interactions [1].

This is not the right place where to discuss the precision tests of the standard model and we only summarize few basic facts. In principle we still have some minor problem in understanding the results of the fits to the experimental data, essentially we would like to understand when the  $\chi^2(M_H)$  shape is unstable with respect to normal fluctuations of the experimental data in the large  $M_H$  tail. Also it appears that some clash between the LEP data and the SLD left-right asymmetry is still present, however for the first time in the LEP 1 history the  $\chi^2_{min}(M_H)$  has overcome some previous and unnatural tendency to be in the forbidden region,  $M_H < 65$  GeV, thus requiring the unnatural introduction of yet another penalty function. After the new results for  $R_{b,c}$  the goodness of the fit has considerably improved upon the past and now the minimal standard model and the minimal supersymmetric standard model are, more or less, on equal footing in describing the experimental results.

At any rate and roughly speaking one could make the following observations: it is still premature to give something more precise than an approximate upper bound on the Higgs boson mass of 500 GeV at 95% of CL. Indeed as a result of the our fit [2] we find

$$\begin{aligned} M_H &= 143.5 \text{ GeV} \\ M_H &\leq 431 \text{ GeV} \quad \text{at} \quad 95\% \quad \text{CL.} \end{aligned} \tag{1}$$

Our predictions for various quantities at the value of the Higgs boson mass corresponding to the minimum of the  $\chi^2$ -distribution are shown in table 1.

However with the indication from the LEP 1 and SLD data – augmented with  $1 - M_W^2/M_Z^2$  from  $\nu N$ -scattering, the  $W$  mass from collider data and  $m_t$  from CDF and D0 – and the advent of LEP 2 we should perhaps stop worrying about Tails&Fits and we should instead start to understand how a Higgs boson - in the LEP 2 energy range - looks like in a real environment citeexp. Indeed in the near future LEP 2 will be the only opportunity for a direct search of a Higgs boson of mass  $> 65$  GeV.

For the first time at LEP most of the events in the  $e^+e^-$  annihilation will have four fermion in the finals state and we have the unique opportunity of testing a complete calculation with the experimental data, well beyond the usual approximation of computing production cross section  $\times$  branching ration of Higgs into decay products. Of course, given the fact that the number of collected events at LEP 2 will be limited and because of the low statistics one could proceed with a well defined strategy: for discovery physics sophisticated tools are unnecessary. However we do have precise theoretical calculations [4] at our disposal already now and it is extremely interesting and appealing to apply our machinery to an analysis – as complete as possible – of the Higgs physics. With an increasing degree of complexity one goes through the following ladder of approximations

Observables	Exp.	Theory	Comments
$M_H$ (GeV)	$> 65$ GeV	143.5 (fixed)	$< 431$ at 95% CL
$\chi^2$		18.22/13	
$m_t$ (GeV)	$175 \pm 6$	$172 \pm 5$	penalty in the fit
$\alpha_{light}^{-1}(M_Z)$	$128.89 \pm 0.09$	$128.905 \pm 0.087$	
$\alpha_s(M_Z)$	–	$0.1194 \pm 0.0037$	th. err. not included
$m_b$ (GeV)	$4.7 \pm 0.2$	$4.68 \pm 0.24$	
$R_l$	$20.778 \pm 0.029$	$20.754 \pm 0.025$	
$\sin^2 \theta_{eff}^e$	$0.23061 \pm 0.00047$	$0.23159 \pm 0.00022$	
$R_b$	$0.2178 \pm 0.001144$	$0.2158 \pm 0.0002$	correlated
$R_c$	$0.1715 \pm 0.005594$	$0.1723 \pm 0.0001$	”
$M_W$ (GeV)	$80.356 \pm 0.125$	$80.350 \pm 0.031$	
$A_{FB}^0(b)$	$0.0979 \pm 0.0023$	$0.1026 \pm 0.0012$	

Table 1: Theory versus Experiments – a fit at the  $Z$  resonance.

- $e^+e^- \rightarrow Z^*H^*$ , followed by the decays  $Z^* \rightarrow \bar{f}f$  and  $H^* \rightarrow \bar{b}b$ . Under the assumption that the Higgs production at LEP 2 is dominated by the Higgsstrahlung process  $e^+e^- \rightarrow Z^* \rightarrow ZH$  the latter factorization is justified by the small Higgs width but the former one is not good enough because of the much larger  $Z$  width. Differential distributions are not accessible. The additional diagrams leading to the same final state are not available.
- $e^+e^- \rightarrow \bar{f}fH^*$ , followed by the decay  $H^* \rightarrow \bar{b}b$ . This works under the hypothesis that the c.m. energy is such that the fusion diagrams can be neglected. Again differential distributions are not accessible. The additional diagrams leading to the same final state are not available.
- The full tree-level calculation  $e^+e^- \rightarrow \bar{b}b\bar{f}f$ . No approximation is made, differential distributions are available and the background is under control (with some limitations to be discussed below).

For a complete discussion of the Higgs boson branching ratios, inclusive of their radiative corrections, we refer to [6] and to references therein.

First of all we have learned how to deal with unstable particles in a fully satisfactory field theoretical context [7], thus the properties of the Higgs boson at LEP 2 can and should be inferred from the analysis of the following processes:

$$\begin{aligned}
e^+e^- \rightarrow & \bar{b}b\mu^+\mu^-, & \bar{b}be^+e^-, \\
& \bar{b}b\bar{\nu}\nu, & \bar{b}b\bar{u}u, (\bar{c}c), \\
& \bar{b}b\bar{d}d, (\bar{s}s), & \bar{b}b\bar{b}b.
\end{aligned} \tag{2}$$

with all the complications arising from flavor mis-identification. Thus the three typical signatures are

1. two jets + a charged lepton pair,
2. two jets + missing energy and momentum,
3. four jets

Thus our aim is to provide predictions for these processes at the partonic level, giving useful informations on the strategy for Higgs searches and on the relative importance of the background to the Higgs signal. The ideal procedure would be to analyze all the above channels with some event generator - the ultimate one - which should

- account for the experimental setup, optimized for the search of the Higgs boson,
- include a self-consistent set of radiative corrections [8], to optimize the theoretical accuracy,

- be interfaced with standard hadronization packages [9].

A broad separation can be set between the two alternative poles: a dedicated electroweak calculations or a general purpose simulations. In this context a crucial role is played by the hadronization process [9].

At least in first approximation we could say that a dedicated electroweak calculation will describe the electroweak content of the processes to very high accuracy but it will lack perturbative parton shower or non-perturbative hadronization. This raises the question of its reliability for the study of hadronic or mixed hadronic-leptonic final states. Even though a pragmatic solution, adopted by many authors, consists in standard interfacing with parton-shower and hadronization programs we still insist on the importance of presenting the most precise predictions for cross sections and distributions with the inclusion of final states QCD perturbative corrections.

It has been shown by the LEP 1 collaborations that such predictions are indeed of the utmost importance for understanding the underlying physical properties of the model once the proper de-convolution procedure is applied to the data. For this reason we are still thinking that a correct (theoretical) treatment of the problem at the level of exact and full matrix elements (including perturbative QCD corrections) will be essential in understanding several features, not least the quantitative effect of some of the most common approximations and the relevance of background versus signal, all of this in presence of some set of simple but realistic enough cuts.

Therefore we want to discuss the Higgs boson properties at LEP 2 by including all diagrams for all given channels at the 0.1% level of technical precision (or better) and by including the best available set of corrections, i.e. initial state QED radiation through the structure function approach [11], running quark masses [12], naive QCD (NQCD) final state corrections.

When using the exact matrix elements it becomes desirable to include final state QCD corrections, even when kinematical cuts are imposed on the outgoing fermions. Lacking a complete calculation we have adopted in this paper the so called naive approach where by naive QCD we mean a simple recipe where the total  $H(Z)$ -width and the cross section are corrected by some simple multiplicative factors. This naive approach, consequence of our ignorance about the complete result, would be correct only for the double-resonant diagrams within a fully extrapolated setup.

One final comment is in order here on the general philosophy of our approach, which is shared by many other authors already present in the literature. To a large extent the standard Higgs boson – being such a narrow resonance – could be considered as an almost stable particle and one could be tempted and motivated in investigating independently its production mechanism and its decay processes. One more requirement has to be fulfilled in this respect, the Higgs boson physics must be something to be added incoherently to the background. As already noticed in the massless limit signal and background add incoherently but there are production mechanisms, say for  $e^+e^- \rightarrow \bar{b}b\bar{\nu}_e\nu_e$ , where different contributions have an interference, typically the fusion process with the Higgsstrahlung one. Since  $\bar{b}b$ + neutrinos represent 20% of the signal at LEP 2 energies this has to be correctly taken into account as described elsewhere in this paper with the global description of the Higgs-fusion relevance as a function of the kinematical cuts.

To understand the general degree of complexity of the calculation based on the full matrix element approach we have shown in table 2 a simple counting of the diagrams which occur in all processes.

Final state	Class/max # of diagrams
$\bar{b}b\mu^+\mu^-$	NC25
$\bar{b}be^+e^-$	NC50
$\bar{b}b\bar{\nu}_\mu\nu_\mu$	NC25
$\bar{b}b\bar{\nu}_e\nu_e$	NC21
$\bar{b}b\bar{u}u, (\bar{c}c)$	NC33
$\bar{b}b\bar{d}d, (\bar{s}s)$	NC33
$\bar{b}b\bar{b}b$	NC68

Table 2: Diagrams required (including gluons) for the process  $e^+e^- \rightarrow \bar{b}b\bar{f}f$ .

Our terminology is an obvious extension of the one introduced in [4]. Thus NC-type refers to the production of two fermion-antifermion pairs  $(\bar{F}_i, f_i) + (\bar{F}_j, f_j)$  where  $i, j$  are generation indices. To give an example NC50 is the natural extension of NC48 with two extra diagrams corresponding to Higgstrahlung and  $ZZ$  fusion. Here all the processes are of the Neutral Current type (NC) and in  $\bar{b}b\bar{b}b$  we have neglected those diagrams which correspond to a  $\bar{b}b$  pair production from a  $b(\bar{b})$  leg. Moreover in the massless limit the interference between the Higgs signal and its background is zero, fact which greatly simplifies the calculation. This is a consequence of the coupling of massless fermions to either spin-vectors or to the Higgs, a spin-scalar.

Thus the strategy for the calculation is relatively simple. There are already several examples of Higgs studies in the literature which have addressed and solved several important issue. It is rather difficult to summarize all the work done in the recent past. Tentatively we point out the relevance of the pioneering work of E. Boos and M. Dubinin [13] on the Monte Carlo calculation of the processes

$$\begin{aligned}
 e^+e^- &\rightarrow Z\bar{b}b, \\
 e^+e^- &\rightarrow \bar{b}b\mu^+\mu^-.
 \end{aligned}
 \tag{3}$$

The same process has been extensively analyzed by G. Montagna, O. Nicrosini and F. Piccinini [21]. Also we stress the importance of the semi-analytical approach to Higgs production at LEP 2, as illustrated by the work of D. Bardin, A. Leike and T. Riemann [14]. Important contributions to understand Higgs physics - even though not from the point of view of LEP 2 energy range - can be found in the work of P. Grosse-Wiesmann, D. Haidt and J. Schreiber [15] and in the one of P. Janot [16].

A complete and exhaustive comparison for Higgs physics can be found in the Report of the Workshop in Physics at LEP 2, where the signal and background cross sections for the process  $e^+e^- \rightarrow \bar{b}b\mu^+\mu^-$  have been compared among the following FORTRAN codes: CompHEP [17], EXCALIBUR [18], FERMISV [19], GENTLE/4fan [20], HIGGSPV [21], HZHA/PYTHIA [22], WPHACT [23] and WTO [24]. It should be stressed that during this comparisons no QCD corrections have been applied and the  $b$ -quark mass has been fixed to its pole value. In this respect our results represent another step towards the ultimate Higgs prediction.

Other codes designated for 4-fermion physics have been quite active recently. In the previous list we have only quoted the participants in the Higgs physics working group at the LEP 2 workshop who have actually produced results for the published tables. For further general references one should consult ref. [25].

Among the most recent analyses we would like to quote the work of Katsanevas and collaborators [26] who present a study of  $e^+e^- \rightarrow \bar{b}b\bar{\nu}\nu$  at c.m. energies  $150 \leq \sqrt{s}(\text{GeV}) \leq 240$  and where the important differential distributions for the Higgs boson and the background components are studied, providing information useful for choosing cuts in Higgs searches.

In this paper we present a modest contribution to the discussion by analyzing many different final states which are important for the discovery of a minimal standard model Higgs boson at LEP 2. This we will do in one study, without selecting any particular signature and by using the FORTRAN code WTO [24].

Although the issue of the fermion masses will be addressed later in the paper here we stress that all the reported results are computed with massless fermions, Yukawa couplings excluded. Masses are not a limitation of principle in the formalism upon which WTO is based but they are not yet implemented, thus we refer to those code which have already produced results with  $m_b \neq 0$ , noticeably CompHEP [17], and WPHACT [23]. Also we will devote little space to  $\bar{b}b\bar{b}b$  final states and signal where, to the best of our knowledge, the most reliable results are achievable with WPHACT.

The outline of the paper is as follows. In sect 2 we present and discuss in details our strategy for the calculation. In sect. 3 we briefly discuss the theoretical uncertainties associated with the formulation of the problem and with the choice of the input parameters. The presentation of all processes, their background and of the set of kinematical cuts is in sect. 4 while a detailed discussion of the numerical results is contained in sect. 5. Our conclusions are shown in sect. 6.

## 2 Strategy of the calculation

In this section we will show how the calculation of the Higgs boson signal and of its background is organized. At the same time the feasibility of the approach will be illustrated.

All fermions masses which occur in

$$e^+e^- \rightarrow \bar{b}b\bar{f}f, \quad (4)$$

are neglected but for the  $b$ -quark mass in the Yukawa coupling and for the  $b$ -quark,  $c$ -quark and  $\tau$  masses in the decay width. Quark masses are running and evaluated according to [12]

$$\begin{aligned} \bar{m}(s) &= \bar{m}(m^2) \exp \left\{ - \int_{a_s(m^2)}^{a_s(s)} dx \frac{\gamma_m(x)}{\beta(x)} \right\}, \\ m &= \bar{m}(m^2) \left[ 1 + \frac{4}{3} a_s(m) + K a_s^2(m) \right], \end{aligned} \quad (5)$$

where  $m = m_{pole}$  and  $K_b \approx 12.4$ ,  $K_c \approx 13.3$ .

To summarize we have neglected the fermion masses in the phase space while keeping them in the Yukawa couplings. The effect of including the masses in some effective approximation will be discussed later in the paper. The Higgs width is computed with the inclusion of the  $H \rightarrow gg$  channel. The most complete treatment will therefore start with some input value for  $\alpha_s(M_W)$  and it will evolve  $\alpha_s$  to the scale  $\mu = M_H$ , will evaluate the running  $b, c$ -quark masses and finally compute

$$\begin{aligned} \Gamma_H &= \frac{G_G M_H}{4\pi} \left\{ 3 \left[ m_b^2(M_H) + m_c^2(M_H) \right] \left[ 1 + 5.67 \frac{\alpha_s}{\pi} + 42.74 \left( \frac{\alpha_s}{\pi} \right)^2 \right] + m_\tau^2 \right\} \\ &+ \Gamma_{gg}, \\ \Gamma_{gg} &= \frac{G_\mu M_H^3}{36\pi} \frac{\alpha_s^2}{\pi^2} \left( 1 + 17.91667 \frac{\alpha_s}{\pi} \right). \end{aligned} \quad (6)$$

As already indicated NQCD is included by evolving  $\alpha_s(M_W)$ (input) to  $\alpha_s(M_H)$  and the Higgs boson signal is multiplied by

$$\begin{aligned} \delta_{QCD} &= 1 + 5.67 \frac{\alpha_s}{\pi} + 42.74 \left( \frac{\alpha_s}{\pi} \right)^2, \\ \alpha_s &= \alpha_s(M_H). \end{aligned} \quad (7)$$

Similarly whenever we consider  $e^+e^- \rightarrow \bar{b}b\bar{q}q$  there will be an additional NQCD correction factor  $1 + \alpha_s/\pi$ , where  $\alpha_s$  is now evaluated at a scale  $\mu = M_Z$ .

Admittedly this is not the most satisfactory solution to the problem of final state QCD corrections. Besides what we have already indicated it must be said that several QCD diagrams (gluon-exchange) are, in this way, neglected. For instance there are multi-leg diagrams, including boxes or even higher. In other words NQCD is equivalent to shrink the whole electroweak part of a diagram to a point and to apply QCD radiation to each  $\bar{q}_i q_i$  pair at a fixed scale –  $\mu = M_H$  for  $\bar{b}b$ ,  $\mu = M_Z$  for the rest – while neglecting at the same time all kinematical cuts. To illustrate the expected properties we have shown in table 3 some of the parameters of the Higgs boson for different values of its mass:

Parameter	$M_H = 80$ GeV	$M_H = 90$ GeV	$M_H = 100$ GeV
$\Gamma_H$	1.8515 MeV	2.0601 MeV	2.2734 MeV
$m_b(M_H)$	2.731 GeV	2.702 GeV	2.676 GeV
$m_c(M_H)$	0.553 GeV	0.547 GeV	0.542 GeV
$\alpha_s(M_H)$	0.12557	0.12323	0.12121

Table 3: Input is  $\alpha_s(M_Z) = 0.123$ ,  $m_b = 4.7$  GeV and  $m_c = 1.55$  GeV.

To continue our description of the chosen strategy we will say that the matrix elements are generated in our calculation through the helicity formalism of ref. [27] and they are compact expressions completely given in terms of the invariants which describe the process. Also the momenta of the final states are, component by component, given in terms of the invariants used in the integration over the phase space, thus allowing to implement the kinematical cuts with an analytical control.

We adopted this procedure to compute all the relevant cross sections with the FORTRAN code WTO<sup>1</sup>. However for a Higgs study all kind of distributions at the parton level are extremely important. For this reason we have extended the original version of WTO in order to allow for the generation of unweighed events and for the storage of their four-momenta. After that all kind of distributions can be analyzed, according to a well established procedure. The full description of WTO 2.0 and of the methods adopted to generate unweighed events will be given elsewhere [29]. For a large number of differential distributions therefore WTO can work under two alternative strategy, a deterministic integration with analytical control over the boundaries of the phase space or an event generator. In the former case a differential distribution can be generated bin by bin with a slow but very precise procedure while in the latter the same distribution is generated in one run with a fast procedure. In a large number of cases we have therefore confronted the results of the two approaches with a quite satisfactory agreement.

Whenever computing processes with a Higgs boson exchange one is usually faced with

---

<sup>1</sup>A preliminary collection of results from WTO for Higgs searches can be found in ref. [28]

the problem of including the fermion masses or not in the calculation. The Yukawa coupling

$$\bar{f}Hf = -\frac{1}{2}g\frac{m_f}{M}, \quad (8)$$

are of course there but usually the fermion mass effects in the rest of the matrix element and in the phase space are neglected. The main reason for doing that has always to do with the CPU time needed for the calculation and, usually is never a matter of principle. In order to understand the corresponding behavior we have investigate an effective mechanism for introducing fermion mass effects. Since the Higgs width is extremely narrow and since the running masses are at most of the order of  $2 \div 3$  GeV we can think of including mass effects in a narrow width approximation. For instance in the  $ZH$  production mechanism and for some fully extrapolated setup we can write the basic off-shell  $ZH$  production as

$$\begin{aligned} \sigma_{ZH}(s) &= \int_0^s ds_1 \rho_H(s_1) \int_0^{(\sqrt{s}-\sqrt{s_1})^2} ds_2 \rho_Z(s_2) \sigma_{ZH}(s; s_1, s_2), \\ \rho_V(s_i) &= \frac{1}{\pi} \frac{\sqrt{s_i} \Gamma_V(s_i) \times BR(i)}{|s_i - M_V^2 + i \sqrt{s_i} \Gamma_V(s_i)|^2}. \end{aligned} \quad (9)$$

In narrow width approximation we multiply the  $e^+e^- \rightarrow \bar{b}b\bar{f}f$  cross section by a factor  $F_{mass}$  given by

$$\begin{aligned} F_{mass} &= \beta^3 \left(1 + \frac{\Gamma_b}{\Gamma_R}\right) \left(1 + \beta^3 \frac{\Gamma_b}{\Gamma_R}\right)^{-1}, \\ \beta^2 &= 1 - 4 \frac{m_b^2(M_H)}{M_H^2}, \\ \Gamma_R &= \Gamma_H - \Gamma_b. \end{aligned} \quad (10)$$

The numerical impact will be discussed in the section about numerical results. In general however our calculation is exact at  $\mathcal{O}(m_b^2(M_H))$  and for this reason in the process  $e^+e^- \rightarrow \bar{b}b\bar{b}b$  we have neglected diagrams which correspond to a  $\bar{b}b$  pair produced by a  $b(\bar{b})$  line since they give contributions to the cross section of  $\mathcal{O}(m_b^4(M_H))$ .

### 3 Theoretical uncertainties

Each calculation aimed to provide some estimate for 4-fermion production is, at least nominally, a tree level calculation. Among other things it will require the choice of some

set of input parameters and of certain relations among them. This is usually referred in the literature, although improperly, as the choice of the Renormalization Scheme (RS).

So far an attempt to investigate the problem has been performed by GENTLE/4fan and by WTO [4]. More recently the size of the theoretical uncertainties for neutral current processes has been addressed by WPHACT [5] and WTO.

There are several sources for the theoretical uncertainty and no fully reliable estimate of the theoretical error can be given. At most we can produce a rough estimate by applying few options connected with the choices of the Renormalization Scheme.

Typically we have at our disposal four experimental data point (plus  $\alpha_s$ ), i.e. the measured vector boson masses  $M_Z, M_W$  and the coupling constants,  $G_\mu$  and  $\alpha$ . However we only have three bare parameters at our disposal, the charged vector boson mass, the  $SU(2)$  coupling constant and the sinus of the weak mixing angle. While the inclusion of one loop corrections would allow us to fix at least the value of the top quark mass from a consistency relation this cannot be done at the tree level. Thus different choices of the basic relations among the input parameters can lead to different results with deviations which, in some case, can be sizeable.

For instance we have considered the Higgs background ( $M_H = \infty$ ) at one particular energy, 190 GeV, and computed the corresponding cross sections in two among the most popular schemes. This background is therefore affected by the theoretical error shown in table 4.

Process	1-( $G_F$ scheme)/( $\alpha$ scheme) (permill)
$\bar{b}b\bar{\nu}_\mu\nu_\mu$	0.86
$\bar{b}b\mu^+\mu^-$	2.23
$\bar{b}b\nu_e\nu_e$	2.44
$\bar{b}be^+e^-$	8.05
$\bar{b}b\bar{u}u$	-3.21
$\bar{b}b\bar{d}d$	-3.03

Table 4: Differences (in permill) induced by different Renormalization Schemes for the Higgs background at 190 GeV.

Roughly speaking we can say that the theoretical uncertainty associated with the choice of the RS is most severe whenever low- $q^2$  photons dominate, both for  $q^2 > 0$  and  $q^2 < 0$ . Indeed we have for the most popular choices

- The  $\alpha(M_Z)$  scheme.

$$s_w^2 = \frac{\pi\alpha}{\sqrt{2}G_\mu M_w^2}, \quad g^2 = \frac{4\pi\alpha}{s_w^2} \quad (11)$$

- The  $G_\mu$  scheme

$$s_w^2 = 1 - \frac{M_w^2}{M_Z^2}, \quad g^2 = 4\sqrt{2}G_\mu M_w^2. \quad (12)$$

Thus in the  $G_\mu$ -scheme the e.m. coupling is governed by  $\alpha = 1/131.22$  while in the  $\alpha(M_Z)$ -scheme it is  $\alpha = 1/128.89$  which accounts for a 2% difference. This will propagate into approximately a 10% difference between the two schemes at low- $q^2$  for diagrams with two photons. Processes with both time-like or space-like photons are therefore severely affected unless protective cuts are imposed. For this reason the effect is larger in  $e^+e^- \rightarrow \bar{b}b e^+e^-$ , due to the presence of a multi-peripheral diagram with photons in the  $t$ -channel.

Essentially we may distinguish between  $s$ -channel photons where the difference between the two schemes can be made arbitrarily negligible by cutting on the corresponding  $\gamma^* \rightarrow \bar{f}f$  invariant mass and  $t$ -channel photons where one would have to impose more stringent cuts on the corresponding scattering angle.

Actually there is a third alternative, somehow dictated by the LEP 1 framework which in some case could be more relevant. First we compute the running of  $\alpha$  up to a scale  $\mu = M_Z$ . This can be done by including the leptons and the top quark perturbatively while the light quarks are accomodate through dispersion relations [10]. Next we define

$$\begin{aligned} s_w^2 &= \frac{1}{2} \left[ 1 - \sqrt{1 - \frac{4\pi\alpha(M_Z)}{\sqrt{2}G_\mu M_Z^2}} \right] \\ g^2 &= 4\sqrt{2}G_\mu M_Z^2 c_w^2. \end{aligned} \quad (13)$$

Other additional sources of uncertainty are in the parametrization of the QED structure functions [11], in the treatment of the scale  $\mu$  in the QCD corrections, especially so for the scale of  $\alpha_s$  in the NQCD correction factor. The default established during the LEP 2 workshop usually consists in inserting  $\alpha_s$  at fixed  $\mu$  even for internal gluons in a process like  $e^+e^- \rightarrow \bar{b}b\bar{q}q$ . In this case the scale is generally chosen to be  $M_Z$  or  $M_H$ . A better choice could be to use  $\alpha_s$  evaluated at a running virtuality, i.e.  $\alpha_s(\hat{s})$  where for instance  $\hat{s}$  is the invariant mass of the  $\bar{q}q$  pair. With this choice however some lower cuts on the invariant masses are required to avoid the non-perturbative, low- $q^2$ , regime.

On top of the theoretical uncertainties there are additional problems, flavor mis-identification and correct treatment of the background. Experimentally one must extract the Higgs signal from all final states consisting of a pair of (imperfectly)  $b$ -tagged jets +

remaining products (including the missing ones). The probabilities of a light quark, a  $c$ -quark or a  $b$ -quark jet to be confused with a  $b$ -quark are non zero. The effect of flavor mis-identification modifies the original branching ratios. For instance a 2-jet final state  $q_1\bar{q}_2$  with given quark flavors can be characterized by a two-by-two matrix [15]

$$\begin{pmatrix} (1 - P_{1b})(1 - P_{2b}) & (1 - P_{1b})P_{2b} \\ P_{1b}(1 - P_{2b}) & P_{1b}P_{2b} \end{pmatrix}$$

In order to introduce a discussion for the Higgs background we observe that at LEP 2 a large fraction of Higgs events will be of the type  $\bar{b}b\bar{\nu}\nu$  ( $\approx 20\%$ ). There are potentially large backgrounds in the process  $e\nu_e c s$  with flavor mis-identification and with the electron lost in the beam-pipe. A safe estimate requires including  $m_e$  in the calculation since we go down to  $\theta_e = 0$  – zero scattering angle for the electron – where moreover gauge invariance is in danger. Another example is given by  $l^+l^-\bar{b}b$  with the leptons lost in the beam-pipe. Again it requires a finite lepton mass because of divergent multi-peripheral diagrams. No reliable estimate has been given so far in the literature.

To explain in more details the gauge invariance issue we can say that here we are dealing with CC20 diagrams with  $t$ -channel photons which induce an apparent singularity at zero scattering angle. This is of course cured by avoiding the approximation of massless fermions but there is more. Any calculation for  $e^+e^- \rightarrow 4$ -fermions is only nominally a *tree level* approximation because of the presence of charged and neutral, unstable vector bosons and of their interaction with photons.

Unstable particles require a special care and their propagators, in some channels, must necessarily include an imaginary part or in other words the corresponding  $S$ -matrix elements will show poles shifted into the complex plane. In any field-theoretical approach these imaginary parts are obtained by performing the proper Dyson resummation of the relative two-point functions, which at certain thresholds will develop the requested imaginary component. The correct recipe seems representable by a Dyson resummation of fermionic self-energies where only the imaginary parts are actually included. As a result the vector boson propagators will be inserted into the corresponding tree level amplitudes with a  $p^2$ -dependent width. It has already been noticed by several authors [7] that even this simple idea gives rise to a series of inconsistencies, which sometimes may give results completely inconsistent even from a numerical point. The fact is that the mere introduction of a width into the propagators will inevitably result, in some cases, into a breakdown of the relevant Ward identities of the theory with a consequent violation of some well understood cancellation mechanism. In the CC20 case the effect of spoiling a cancellation among diagrams results into a numerical catastrophe. The solution of this apparent puzzle is by now well known and amounts to the inclusion of the so-called Fermion-Loop scheme [7]. A reliable estimate of this background would require the introduction of both a finite electron mass and of the Fermion-Loop scheme. A full description of The Fermion Loop scheme is well beyond the scope of our paper. There are two versions of the scheme, one where roughly speaking one adds the imaginary parts of all fermionic one loop diagrams and a second more complete one which amounts to the

inclusion of the full  $\mathcal{O}(\alpha)$  fermionic corrections, inclusive of the proper treatment of the vector boson complex poles.

## 4 The Higgs signal and its background

In order to analyze the Higgs signal versus background at LEP 2 we fix our set of quasi-realistic cuts for the processes to be considered by WTO. At the parton level they are

1.  $M(\bar{b}b) \geq 50 \text{ GeV}$ ,  $|M(\bar{f}f) - M_z| \leq 25 \text{ GeV}$ . The former is to suppress the photon mediated  $\bar{b}b$  production – which decreases for larger  $\sqrt{s}$ . The latter reduces all contributions which give a broad  $M(\bar{f}f)$  spectrum.
2. Lepton momenta  $\geq 10 \text{ GeV}$ .
3. Quark energies,  $E_q \geq 3 \text{ GeV}$ .
4. Lepton polar angles with the beams  $\geq 15^\circ$ .
5. For processes with neutrinos the angle of both b's with the beams  $\geq 20^\circ$  or of at least one b.
6.  $\theta(l, q) \geq 5^\circ$ .

This set of kinematical cuts is the one chosen during the last LEP 2 workshop and after that it has been termed Canonical Cuts (or CC in shorts). For the  $\bar{b}b\bar{b}b$  final state some additional selection will be introduced in the next section.

We have already pointed out that our prediction are at the parton level and moreover any realistic analysis will require several further acceptance criteria,  $b$ -tagging and constrained morphology. Detecting a Higgs boson at LEP 2 requires also the isolation of the signal from many different sources of electroweak background. They have been classified recently in ref. [26] and here we would like to spend few more words of comment.

- $s$ -channel production of  $\bar{b}b$  jets with soft and undetected hadrons. This is a long-standing problem of the separation between 4-fermion final states from what one should really consider as radiative corrections – initial state pair production – to 2-fermion final states at LEP 2. Here any calculation requires experimental guidance on the set of cuts needed to distinguish the two regimes. In principle there should be little problem in interfacing 2-fermion codes with 4-fermion codes in order to give a correct treatment of the relevant physical processes at LEP 2. <sup>2</sup>
- $e^+e^- \rightarrow cs\nu\tau (\rightarrow \nu\bar{\nu} + \text{soft charged particles})$ . This is a typical CC10 process which is well under control even though the existing dedicated electroweak codes should be interfaced with some  $\tau$ -decay library.

---

<sup>2</sup>The interfacing of TOPAZ0(2f) with WTO(4f) is currently under investigation

- $e^+e^- \rightarrow e\nu_e cs$  with flavor mis-identification and the  $e$  lost in the beam-pipe or  $e^+e^- \rightarrow l^+l^-\bar{b}b$  with the leptons lost in the beam-pipe. We have already indicated that no reliable estimate has been performed so far. Take for instance the typical CC20 process  $e^+e^- \rightarrow e\nu_e cs$ , here gauge invariance becomes essential in the region of phase space where the scattering angle of the electron is small and moreover in the same region the photon propagator behaves like  $1/m_e^2$ . Thus both finite electron mass and  $U(1)$  gauge invariance are required for a meaningful cross section with the outgoing electron contained in a small cone around the beam axis.

## 5 Numerical Results and Comments

To understand the Higgs boson search at LEP 2 through the subprocess contributions to the cross section as functions of the c.m. energy we have reported in figure 1 the cross sections for  $e^+e^- \rightarrow \bar{b}b\bar{f}f$  where  $f = \mu, \nu_\mu$  ( $HZ$ -component),  $f = \nu_e$  ( $HZ + WW$ -components) and  $f = e$  ( $HZ + ZZ$ -components).

In this figure we have shown both the complete cross sections as well as the differences  $\sigma - \sigma_{bckg}$  (where  $bckg$  indicates the same process but with  $M_H = \infty$ ) which illustrate how the  $ZZ$  component is much less relevant than the  $WW$  one, which in turns is not negligible over the whole LEP 2 energy range. The relative importance of the  $WW$ -component, below the  $HZ$  threshold, around it and slightly above is illustrated in figure 2 where we have compared  $3\sigma(e^+e^- \rightarrow \bar{b}b\bar{\nu}_\mu\nu_\mu)$  with  $3\sigma(e^+e^- \rightarrow \bar{b}b\bar{\nu}_\mu\nu_\mu) + \sigma(e^+e^- \rightarrow \bar{b}b\bar{\nu}_e\nu_e)$ .

To continue the discussion of our results we start from the evaluation of the cross sections as a function of  $\sqrt{s}$  for  $M_H = 80$  GeV, 90 GeV, 100 GeV and  $\infty$ . They are show in figure 3. Whenever a process is indicated it has to be understood that the reference kinematical cuts, as described in the previous section, are applied. Our findings confirm the rule of thumb

$$M_H \approx \sqrt{s} - 100 \text{ GeV for LEP 2 feasibility}$$

It is indeed evident that for the cross sections the ratio signal/background, for fixed  $M_H$ , has a maximum at  $\sqrt{s} \approx M_H + 100$  GeV. If the Higgs is above 80 GeV then the cross section is too small at  $\sqrt{s} = 175$  GeV to allow for a Higgs discovery, thus the  $\sqrt{s} = 190$  GeV phase of the collider – or a higher one – will be needed. Moreover at  $\sqrt{s} \geq 190$  GeV the  $ZZ$  background is not negligible and here is where a dedicated EW calculation becomes useful. For instance we assume a Higgs mass of 100 GeV and compare  $\sigma(\text{signal})$  versus  $\sigma(\text{background})$  at 195 GeV. The effect of the background is clearly shown in table 5 to be of the order of 50%.

Another point where a dedicated electroweak calculation indeed makes substantial improvement is given by the process  $e^+e^- \rightarrow \bar{b}b\bar{\nu}_e\nu_e$  process because of the presence of  $t$ -channel diagrams. It has already been reported in ref. [4] that for  $\sqrt{s} = 175$  GeV and – for instance  $M_H = 90$  GeV – the difference between HZHA and the average among HIGGSPV, WPHACT and WTO is approximately 42%, in a situation where the agreement between the dedicated Higgs codes is systematically better than 1%. Having or not control over the full set of diagrams clearly makes a difference.

Process	$\sigma(\text{signal})$	$\sigma(\text{background})$
$\bar{b}b\bar{\nu}_\mu\nu_\mu$	24.957	16.439
$\bar{b}b\mu^+\mu^-$	13.515	9.205
$\bar{b}b\nu_e\nu_e$	29.068	16.874
$\bar{b}be^+e^-$	15.631	11.449
$\bar{b}b\bar{u}u$	51.110	34.276
$\bar{b}b\bar{d}d$	63.924	42.277

Table 5: Signal versus Background cross sections in fb. The c.m. energy is 195 GeV.

A word of comment is needed at this point, it is important to point out that the impact of the discrepancies is minimal on the discovery potential of LEP 2. However when we come to the question of the extraction of Higgs properties then the perspective changes, control on the exact matrix elements is required to eliminate the largest discrepancies and the effect of additional % level uncertainties – of the order of those coming from higher order corrections – will require further work to be fully understood.

Coming back to the cross sections they will be shown later on in several figures but – for further reference and for comparisons – we have also shown a reduced sample of results in table 6.

At this point we also present results for the cross section relative to the process  $e^+e^- \rightarrow \bar{b}b\bar{b}b$ . Within our approximations, which have already been described in the paper, we have adopted two different algorithms.

A1 In the first one all the  $bb$  and  $\bar{b}b$  pairs are required to have an invariant mass of at least 30 GeV to suppress the gluonic and photonic components.

A2 In the second we have adopted the following algorithm. Let  $M_{ij}$  be the invariant mass of the final state  $i - j$  pair ( $i, j = 1, 4$ ), then we define  $M_i$  ( $i = 1, 6$ ) by

$$\begin{aligned}
M_1 &= M_{12}, & M_2 &= M_{34}, \\
M_3 &= M_{13}, & M_4 &= M_{24}, \\
M_5 &= M_{14}, & M_6 &= M_{23}.
\end{aligned} \tag{14}$$

Next we always require  $M_i \geq 5 \text{ GeV}$  and we further apply the rule

Process/ $M_H$ (GeV)	80	90	100	$\infty$
$\sqrt{s} = 175$ GeV				
$\bar{b}b\bar{\nu}_\mu\nu_\mu$	17.519(1)	1.5849(8)	0.9905(8)	0.9082(8)
$\bar{b}b\mu^+\mu^-$	9.243(1)	1.1291(8)	0.8265(8)	0.7851(7)
$\bar{b}b\nu_e\nu_e$	22.570(2)	3.3981(8)	1.2797(8)	0.7489(8)
$\bar{b}be^+e^-$	10.047(2)	2.120(2)	1.870(2)	1.832(2)
$\bar{b}b\bar{u}u$	36.30(1)	4.364(5)	3.171(4)	3.010(4)
$\bar{b}b\bar{d}d$	45.44(1)	4.412(3)	2.878(3)	2.677(3)
$\sqrt{s} = 190$ GeV				
$\bar{b}b\bar{\nu}_\mu\nu_\mu$	42.154(4)	30.430(2)	14.9913(6)	-
$\bar{b}b\mu^+\mu^-$	22.339(3)	16.213(1)	8.330(1)	-
$\bar{b}b\nu_e\nu_e$	47.062(5)	34.635(2)	17.6166(9)	-
$\bar{b}be^+e^-$	24.646(6)	18.290(7)	10.380(6)	-
$\bar{b}b\bar{u}u$	86.72(6)	62.43(7)	31.16(7)	-
$\bar{b}b\bar{d}d$	109.8(1)	78.6(1)	38.4(1)	-

Table 6: Cross sections in fb for  $e^+e^- \rightarrow \bar{b}b\bar{f}f$ . The kinematical cuts have been given explicitly in the previous section.

- if  $\{|M_1 - M_Z| < 25 \text{ GeV}, M_2 > 50 \text{ GeV}\}$ .or.  $\{|M_2 - M_Z| < 25 \text{ GeV}, M_1 > 50 \text{ GeV}\}$  then the event is accepted
- else if  $\{|M_3 - M_Z| < 25 \text{ GeV}, M_3 > 50 \text{ GeV}\}$ .or.  $\{|M_4 - M_Z| < 25 \text{ GeV}, M_3 > 50 \text{ GeV}\}$  then the event is accepted
- else if  $\{|M_5 - M_Z| < 25 \text{ GeV}, M_6 > 50 \text{ GeV}\}$ .or.  $\{|M_6 - M_Z| < 25 \text{ GeV}, M_5 > 50 \text{ GeV}\}$  then the event is accepted
- else the event is rejected.

For a  $M_H = 80, 90 \text{ GeV}$  the corresponding cross sections are shown in table 7 where the first entry refers to A1 and the second to A2.

$\sqrt{s} \text{ (GeV)}/M_H \text{ (GeV)}$	80	90
160	1.973	1.486
	5.050	4.078
165	2.713	1.730
	6.706	4.959
170	6.004	2.122
	12.181	6.006
175	22.592	2.924
	38.665	7.858
180	30.995	6.342
	54.133	38.555

Table 7: Cross sections (fb) for  $e^+e^- \rightarrow \bar{b}b\bar{b}b$ . The first entry correspond to the selection  $M_{ij} \geq 30 \text{ GeV}$  while the second one refers to the algorithm described in the text.

There are several differential distributions which are of some relevance in the Higgs study. They provide informations useful for choosing cuts in the Higgs searches. Among them we have selected:

- The  $M(\bar{b}b)$  distribution for all channels but  $\bar{b}b\bar{b}b$ . It is useful whenever the direct reconstruction of the invariant mass from the jets in the process is viable.
- The  $M(\bar{f}f)$  distribution, in particular – but not only – the  $M(\bar{\nu}\nu)$  one.
- The missing mass recoil. A knowledge of  $\sqrt{s}$  and of the leptonic final states is required

$$M_{rec}^2 = s - 2\sqrt{s}(E_{l^+} + E_{l^-}) + M^2(l^+l^-) \quad (15)$$

- The visible energy in  $\bar{b}b\nu\nu$ , or in general  $E(\bar{b}) + E(b)$ . The  $b$ -quark pairs from the Higgs decay have a sharp peak in the energy distribution due to the small Higgs width.
- Angular distributions for the  $b$ -quark and/or the  $\bar{b}$ -quark. In particular the  $\cos\theta(\bar{b}b)$  distribution of the total 3-momentum  $\vec{p}_{\bar{b}b}$ . However, in general, the signal angular distributions are very isotropic.

Some care has been devoted in understanding qualitatively the effect of flavor mis-identification. For instance we have considered the process

$$\begin{aligned} e^+e^- &\rightarrow \mu^-\mu^+b\bar{b}, \\ e^+e^- &\rightarrow \nu_\mu\bar{\nu}_\mu b\bar{b}. \end{aligned} \quad (16)$$

In absence of flavor identification one has to consider more processes which are subsequently weighted with some external probability. For instance we have assumed the following weights [15]

$$\begin{aligned} e^+e^- \rightarrow \mu^-\mu^+ & \quad b \quad \bar{b}, & P_{bb}^2 &= 0.4665, \\ & \quad d \quad \bar{d}, & P_{db}^2 &= 0.0014, \\ & \quad s \quad \bar{s}, & P_{sb}^2 &= 0.0029, \\ & \quad u \quad \bar{u}, & P_{ub}^2 &= 0.0014, \\ & \quad c \quad \bar{c}, & P_{cb}^2 &= 0.0818, \end{aligned} \quad (17)$$

or

$$\begin{aligned} e^+e^- \rightarrow \nu\bar{\nu} & \quad b \quad \bar{b}, & P_{bb}^2 &= 0.4665, \\ & \quad d \quad \bar{d}, & P_{db}^2 &= 0.0014, \\ & \quad s \quad \bar{s}, & P_{sb}^2 &= 0.0029, \\ & \quad u \quad \bar{u}, & P_{ub}^2 &= 0.0014, \\ & \quad c \quad \bar{c}, & P_{cb}^2 &= 0.0818. \end{aligned} \quad (18)$$

The above probabilities are just for an indication of the general idea which we have illustrated. The gross features of the differential distributions can be understood from

the structure of the sharp peaks around different values of different invariant masses. Typically the narrow width of the Higgs boson will be reflected by an unmistakable peak at  $M(\bar{b}b) = M_H$ . It goes without saying that our predictions are at the partonic level and that the experimental resolution (energy of the  $b$  quarks, angles etc.) has not been included. The latter when properly included will inevitably reduce this rather spectacular peak.

From the full set of diagrams contributing to different channels we have peaks around zero values of some invariant mass due to the sub-processes  $\gamma^*(g) \rightarrow \bar{f}f$  which are usually eliminated by cutting the low values of that variable. We also have peaks in invariant masses around  $M_Z$  due to  $Z^* \rightarrow \bar{f}f$  which becomes dominant whenever the energy becomes larger and larger and the  $ZZ$  background component increases.

There are also peaks around the beam axis due to  $t$ -channel diagrams as the already mentioned multi-peripheral contributions in  $e^+e^- \rightarrow \bar{b}b e^+e^-$ . Finally we do not attribute any particular relevance to a separation of the Higgs signal into Higgsstrahlung or fusion components, they are both present in any complete calculation.

For all processes  $e^+e^- \rightarrow \bar{b}b \bar{f}f, f \neq b$  we have shown the  $M(\bar{b}b)$  distribution for  $\sqrt{s} = 175$  GeV,  $M_H = 80$  GeV while for  $\sqrt{s} = 190$  GeV we have considered three values of the Higgs boson mass,  $M_H = 80, 90$  and  $100$  GeV. They are given in figure 4 through figure 7.

The relative importance of the ratio signal/background from the point of view of the  $M(\bar{b}b)$  distribution is given for a Higgs of 80 GeV and  $\sqrt{s} = 190$  GeV, in figure 8.

Flavor mis-identification has been analyzed in figure 9 and 10 where we have considered  $e^+e^- \rightarrow \mu^+\mu^-(\bar{\nu}_\mu\nu_\mu)\bar{q}q$ . They clearly show the reduction of the  $\bar{b}b$  signal and the contamination around  $M(\bar{q}q) = M_Z$  from the  $\bar{c}c$  mis-identification, the rest remaining negligible.

The ratio signal/background is better illustrated in terms of other differential distributions, typically  $M_{miss}$  or  $E_{\bar{b}+b}$ . Usually the  $M_{miss}$  distribution is used for  $e^+e^- \rightarrow \bar{b}b l^+l^-$  only but we have also shown its behavior for  $e^+e^- \rightarrow \bar{b}b \bar{q}q$  in a situation where exact flavor identification is assumed and  $M(\bar{b}b) \geq 50$  GeV,  $|M(\bar{q}q) - M_Z| \leq 25$  GeV. As it appears the  $b$ -quark pairs from the Higgs decay have a sharp peak in the energy distribution due to the small Higgs width.

For all processes  $e^+e^- \rightarrow \bar{b}b \bar{f}f, f \neq b, \nu$  we have shown the  $M_{miss}$  distribution for  $\sqrt{s} = 175$  GeV,  $M_H = 80$  GeV and for  $\sqrt{s} = 190$  GeV,  $M_H = 80, 90$  and  $100$  GeV. They are given in figure 11 through figure 14. Similarly for all  $f \neq b$  – thus assuming flavor identification – we have shown the energy distribution in figure 15 through figure 18.

The signal/background ratio is given in terms of  $M_{miss}$  and of the  $b$ -quark energies in figure 19 and in figure 20. Finally we have reported in figure 21 the differential distribution in  $\cos\theta_H$ , where  $\theta_H$  is the angle formed by  $\vec{p}(\bar{b}) + \vec{p}(b)$  with the beam direction. As anticipated one can see that, in general, the signal angular distributions are very isotropic for all channels.

A final comment has to be devoted to the effective inclusion of the  $b$ -quark mass. Using the approximate formulation of eq. 10 we have estimated this effect by considering the  $M(\bar{b}b)$  distribution in  $e^+e^- \rightarrow \bar{b}b \bar{\nu}_e \nu_e$  at  $\sqrt{s} = 175$  GeV and  $M_H = 80$  GeV. The deviation of the ratio (effective mass)/(massless) from one for this quantity is of the order of 0.1% around  $M(\bar{b}b) = M_H$  and hardly noticeable away from it. As for the cross section we

have taken the process  $e^+e^- \rightarrow \bar{b}b\mu^+\mu^-$  and compared the effective mass treatment with the massless case in table 8. With respect to the results presented by CompHEP and WPHACT in ref. [4], which take  $m_b$  exactly into account, it should be said that they use  $m_b = m_b(\text{pole}) = 4.7 \text{ GeV}$  in the matrix elements while here  $m_b(80 \div 90 \text{ GeV}) \approx 2.7 \text{ GeV}$ . The choice of ref. [4] is the standard one which was agreed upon and used during the LEP 2 workshop. Of course no general statement can be made here about the full  $m_b$ -mass dependence and to a large extent the size of the effect is deeply related to the particular channel under examination and on the chosen set of kinematical cuts. Therefore the results shown in table 8 are only valid for the particular setup under consideration and should not be confused with a process independent statement. To the best of our knowledge the general answer is under examination by the authors of WPHACT [5].

$\sqrt{s} \text{ (GeV)}/M_H \text{ (GeV)}$	80	90
175	9.243(1)	1.1291(8)
	9.232(1)	1.1288(8)
	-1.2	-0.3
190	22.339(3)	16.213(1)
	22.320(3)	16.204(1)
	-0.9	-0.6

Table 8: Cross sections (fb) for  $e^+e^- \rightarrow \bar{b}b\mu^+\mu^-$ . The first entry corresponds to massless  $b$ -quarks while the second one refers to the inclusion of  $m_b$  following eq. 10. The last entry gives the relative deviation in permill.

## 6 Conclusions

The combined efforts of many different groups, from Europe to Japan, has shown during the last years that the agreement between the dedicated Higgs codes is systematically better than 1%. Here we are considering those theoretical predictions having control over the full set of diagrams which contribute to a given channel. Our point of view is very simple in this respect, it is important to stress that the impact of the discrepancies between dedicated or general purpose calculations is minimal on the discovery potential of LEP 2.

However there is another important question to be answered, the extraction of Higgs properties from the experimental data. Here the perspectives change since we move from discovery physics to precision physics and a full control on the exact matrix elements is required to eliminate any source of large discrepancies. Once this is done we are left with the effect of additional % level uncertainties which are of the same order of those

coming from higher order corrections. To understand the remaining small discrepancies will require further work.

Although a theoretical error by itself is not a well defined quantity we have attempted some very primitive analysis of the problem, trying to understand the interplay between variations in the results among different renormalization schemes and the choice of the cuts which is more suitable to minimize the corresponding effects.

Our main motivation in this paper has been twofold. First we start from the observation that the presently available ensemble of experimental data is not inconsistent with a (minimal standard model) Higgs boson within the range of LEP 2 energies. Secondly the guidance of the published comparisons for complete calculations on Higgs physics at LEP 2 shows that the achieved technical precision and the level of agreement are more than enough to motivate an extension of the previous work to include a larger number of channels in  $e^+e^- \rightarrow \bar{b}b\bar{f}f$ . Additional work is still needed in order to have full control over the background, especially for the  $\bar{b}b\bar{\nu}\nu$  channel.

From a general point of view there is a need to move beyond the mere calculation of the total cross sections, different kinds of differential distributions must be made available to access the widest information for choosing cuts, for discussing the physics of a Higgs boson with a mass around 90 GeV where the Higgs and the  $Z$  signal become degenerate and for a comprehensive analysis of the various background components. In this respect our attempt has been to enlarge several analyses already published in the literature.

In this context we have considered all channels  $e^+e^- \rightarrow \bar{b}b\bar{f}f$  with  $m_f = 0$  everywhere and  $m_b$  non zero only in the Yukawa coupling. Starting from the matrix elements at the parton level we have computed cross sections and differential distributions for various c.m. energies and (minimal standard model) Higgs boson masses. The logical steps to be followed in this field are

- a** to include the matrix elements for the full 4-fermion process  $e^+e^- \rightarrow \bar{b}b\bar{f}f$  beyond the factorization approximation. For four quarks in the final state QCD processes must be added.
- b** The mass of the  $b$ -quark should in principle be kept in the matrix elements, developing a finite interference between signal and background. In our opinion the relatively small value of  $m_b(M_H)$  is enough to justify the massless approximation.
- c** A description of the basic 4-fermion process beyond the minimal standard model, such as SUSY models [30], should be made available.
- d** After a description of the relevant differential distributions at the parton level the unweighed events with the 4-momenta of all final state particles should be provided in order to process the events by applying analysis cuts.

In our analysis we have fulfilled both - a - and - d - of the previous list. We have also indicated some approximations to be used for a quick estimate of the  $b$ -quark mass effect and discussed their validity. Although unweighed events have actually been generated no effort has been made during this work for a proper interface with the hadronization packages.

The outcome of our work is illustrated by several tables and figures which show the feasibility of the project. Among several technical aspects which we consider as extremely relevant for any detailed discussion of the standard Higgs boson properties the main conclusion reiterates the message that if the Higgs mass is above  $80 \text{ GeV}$  then the cross section is too small at  $\sqrt{s} = 175 \text{ GeV}$  to allow for a Higgs discovery, thus the  $\sqrt{s} = 190 \text{ GeV}$  phase of the collider – or even a higher one – will be needed.

## Acknowledgements

I acknowledge many important discussions with Alessandro Ballestrero and his active contribute in exchanging results prior to their publication. His help was essential in creating the event generator branch of WTO and in a better understanding of some of the sources of theoretical error. Several important discussions with the members of the Higgs Physics and of the Event Generators for Discovery Physics working groups at the recent LEP 2 workshop are acknowledged. I sincerely acknowledge the active contribute of D. Bardin, M. Dubinin, O. Nicosini and R. Pittau in the comparison phase with their codes where we have been able to reach agreement with very high precision results on a sample of processes.

## 7 Figure Captions

Fig. 1 Cross sections (pb) for  $e^+e^- \rightarrow \bar{b}b\bar{f}f$  where  $f = \mu, \nu_\mu$  ( $HZ$ -component),  $f = \nu_e$  ( $HZ + WW$ -components) and  $f = e$  ( $HZ + ZZ$ -components). Here  $M_H = 80 \text{ GeV}$ .

Fig. 2 Cross sections (pb) for  $e^+e^- \rightarrow \bar{b}b\bar{\nu}n$  for  $M_H = 80, 90 \text{ GeV}$ .

Fig. 3 Cross sections (pb) for  $e^+e^- \rightarrow \bar{b}b\bar{f}f$  for  $M_H = 80, 90, 100 \text{ GeV}$  and  $M_H = \infty$ .

Fig. 4 The  $M(\bar{b}b)$  distribution for all processes  $e^+e^- \rightarrow \bar{b}b\bar{f}f, f \neq b$  at  $\sqrt{s} = 175 \text{ GeV}$  and  $M_H = 80 \text{ GeV}$ .

Fig. 5 The same as in Fig. 4 but with  $\sqrt{s} = 190 \text{ GeV}$  and  $M_H = 80 \text{ GeV}$ .

Fig. 6 The same as in Fig. 4 but with  $\sqrt{s} = 190 \text{ GeV}$  and  $M_H = 90 \text{ GeV}$ .

Fig. 7 The same as in Fig. 4 but with  $\sqrt{s} = 190 \text{ GeV}$  and  $M_H = 100 \text{ GeV}$ .

Fig. 8 The  $M(\bar{b}b)$  distribution for all processes  $e^+e^- \rightarrow \bar{b}b\bar{f}f, f \neq b$  at  $\sqrt{s} = 190 \text{ GeV}$  and  $M_H = 80 \text{ GeV}$ . The Higgs boson signal and its background are compared.

Fig. 9 Flavor mis-identification is considered in the process  $e^+e^- \rightarrow \mu^+\mu^-\bar{q}q$  for  $\sqrt{s} = 175 \text{ GeV}$  and  $M_H = 80 \text{ GeV}$ .

Fig. 10 The same as in Fig. 9 but for  $e^+e^- \rightarrow \bar{\nu}_\mu \nu_\mu \bar{q}q$ .

Fig. 11 The  $M_{miss}$  distribution for all processes  $e^+e^- \rightarrow \bar{b}b\bar{f}f, f \neq b, \nu$  at  $\sqrt{s} = 175$  GeV and  $M_H = 80$  GeV.

Fig. 12 The same as in Fig. 11 but with  $\sqrt{s} = 190$  GeV and  $M_H = 80$  GeV.

Fig. 13 The same as in Fig. 11 but with  $\sqrt{s} = 190$  GeV and  $M_H = 90$  GeV.

Fig. 14 The same as in Fig. 11 but with  $\sqrt{s} = 190$  GeV and  $M_H = 100$  GeV.

Fig. 15 The  $E_{\bar{b}+b}$  distribution for all processes  $e^+e^- \rightarrow \bar{b}b\bar{f}f, f \neq b$  at  $\sqrt{s} = 175$  GeV and  $M_H = 80$  GeV.

Fig. 16 The same as in Fig. 15 but with  $\sqrt{s} = 190$  GeV and  $M_H = 80$  GeV.

Fig. 17 The same as in Fig. 15 but with  $\sqrt{s} = 190$  GeV and  $M_H = 90$  GeV.

Fig. 18 The same as in Fig. 15 but with  $\sqrt{s} = 190$  GeV and  $M_H = 100$  GeV.

Fig. 19 The  $M_{miss}$  distribution for all processes  $e^+e^- \rightarrow \bar{b}b\bar{f}f, f \neq b, \nu$  at  $\sqrt{s} = 190$  GeV and  $M_H = 80$  GeV. The Higgs boson signal and its background are compared.

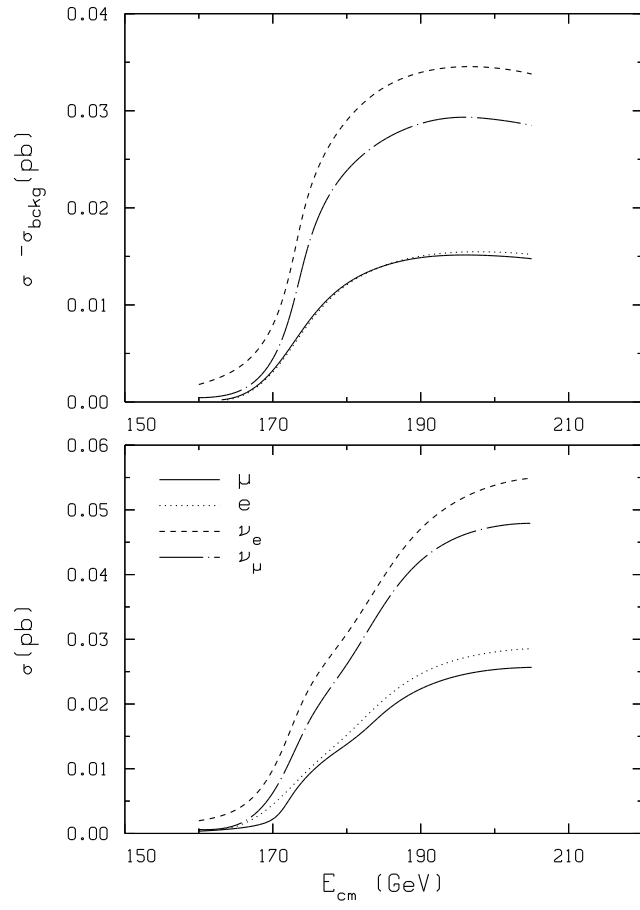
Fig. 20 The  $E_{\bar{b}+b}$  distribution for all processes  $e^+e^- \rightarrow \bar{b}b\bar{f}f, f \neq b$  at  $\sqrt{s} = 190$  GeV and  $M_H = 80$  GeV. The Higgs boson signal and its background are compared.

Fig. 21 The differential distribution in  $\cos\theta_H$  for all processes  $e^+e^- \rightarrow \bar{b}b\bar{f}f, f \neq b$  at  $\sqrt{s} = 175$  GeV and  $M_H = 80$  GeV. Here  $\theta_H$  is the angle formed by  $\vec{p}_{\bar{b}} + \vec{p}_b$  with the beam direction. The Higgs boson signal and its background are compared.

## References

- [1] A. Blondel, talk given at the 28th International Conference on High Energy Physics, Warsaw 1996.
- [2] G. Montagna, O. Nicrosini, G. Passarino, F. Piccinini and R. Pittau, *Comput. Phys. Commun.* 76(1993)328.
- [3] ALEPH Collaboration, CERN-PPE-79;  
DELPHI Collaboration, CERN-PPE-119;  
L3 Collaboration, CERN-PPE-95;  
OPAL Collaboration, CERN-PPE-96.
- [4] *Event Generators for WW Physics* to appear in Vol.1, *Report of the Workshop in Physics at LEP2* G. Altarelli et. al., CERN-96-01;  
*Event Generators for Discovery Physics*, M. L. Mangano et al., to appear in Vol.1, *Report of the Workshop in Physics at LEP2* G. Altarelli et. al., CERN-96-01;  
*Higgs Physics at LEP II*, M. Carena et al., to appear in Vol.1, *Report of the Workshop in Physics at LEP2* G. Altarelli et. al., CERN-96-01.
- [5] A. Ballestrero, private communication.
- [6] A. Djouadi et al., hep-ph/9605437;  
B. Kniehl, hep-ph/9610500.
- [7] W. Beenakker et al. in preparation;  
E. N. Argyres et al., *Phys. Lett.* B358(1995)339;  
R. G. Stuart, *Phys. Lett.* B262(1991)113;  
R. G. Stuart, *Phys. Lett.* B272(1991)353;  
Y. Kurihara, D. Perret-Gallix and Y. Shimizu, *Phys. Lett.* B349(1995)367;  
U. Baur and D. Zeppenfeld, *Phys. Rev. Lett.* 75(1995)1002.
- [8] *WW Cross-Sections and Distributions*, W. Beenakker et al., to appear in Vol.1, *Report of the Workshop in Physics at LEP2* G. Altarelli et. al., CERN-96-01.
- [9] T. Sjöstrand, report of the QCD generators group of the LEP 2 workshop, to appear in Vol.1, *Report of the Workshop in Physics at LEP2* G. Altarelli et. al., CERN-96-01.
- [10] F. Jegerlehner, *Z. Phys.* C32(1986)195;  
H. Burkhardt et al., *Z. Phys.* C42(1989)497;  
S. Eidelman and F. Jegerlehner, *Z. Phys.* C(1995).
- [11] F. A. Berends, R. Kleiss and R. Pittau, *Nucl. Phys.* B426(1994)344;  
G. Montagna, O. Nicrosini and F. Piccinini, *Comp. Phys. Commun.* 90(1995)141;  
G. Montagna, O. Nicrosini, G. Passarino and F. Piccinini, *Phys. Lett.* B348(1995)178.
- [12] K. G. Chetyrkin et al. in *Reports of the Working Group on Precision Calculations for the Z Resonance*, D. Bardin W. Hollik and G. Passarino eds., CERN-95-03, p. 175.

- [13] E. Boos and M. Dubinin, Phys. Lett. 308B(1993)147;  
E. Boos, M. Sachwitz, H. Schreiber and S. Shichanin, Z. Physik C61(1994)675;  
M. Dubinin, V. Edneral, Y. Kurihara and Y. Shimizu, Phys. Lett. B239(1994)379.
- [14] D. Bardin, M. Bilenky, A. Olchevski and T. Riemann, Phys. Lett. B308(1993)403;  
D. Bardin, A. Leike and T. Riemann, Nucl. Phys. B(Proc. Suppl.) 37B(1994)274.
- [15] P. Grosse-Wiesmann, D. Haidt and J. Schreiber in *e<sup>+</sup>e<sup>-</sup> Collisions at 500 GeV: the Physics Potential*, P. M. Zerwas ed., DESY 92-123A, p. 37.
- [16] P. Janot in *e<sup>+</sup>e<sup>-</sup> Collisions at 500 GeV: the Physics Potential*, P. M. Zerwas ed., DESY 92-123A, p. 107.
- [17] E. Boos, M. Dubinin, V. Edneral, V. Ilyin, A. Kryukov, A. Pukhov and S. Shichanin in *New Computing Techniques in Physics Research II*, ed. by P. Perret-Gallix, World Scientific, Singapore, 1992, p. 665.
- [18] F.A. Berends, R. Kleiss and R. Pittau, Comp.Phys.Comm. 85(1995)437;  
Nucl.Phys. B424(1994)308;  
Nucl.Phys. B426(1994)344.
- [19] J. Hilgart, R. Kleiss and F. Le Diberder, Comput. Phys. Commun. 75(1993)191.
- [20] D. Bardin, A. Leike and T. Riemann, Phys. Lett. B344(1995)383;  
D. Bardin, A. Leike and T. Riemann, Phys. Lett. B353(1995)513.
- [21] G. Montagna, O. Nicrosini and F. Piccinini, Phys. Lett. B348(1995)496.
- [22] T. Sjöstrand, Comp. Phys. Comm. 82(1994)74.
- [23] E. Accomando and A. Ballestrero, WPHACT 1.0, hep-ph/9607317, to appear in Comp. Phys. Comm.
- [24] G. Passarino, Comp. Phys. Comm. 97(1996)261.
- [25] T. Ohl, Talk given at the 3rd International Symposium on Radiative Corrections, Cracow, Poland, August 1-5, 1996, to appear in the Proceedings.
- [26] D. Apostolakis, P. Ditsas and S. Katsanevas, hep-ph/9603383.
- [27] G. Passarino, Nucl. Phys. B237(1984)249.
- [28] G. Passarino, Standard Model and Electroweak Interaction: Phenomenology, Talk given at the 3rd International Symposium on Radiative Corrections, Cracow, Poland, August 1-5, 1996, to appear in the Proceedings.
- [29] G. Passarino, WTO 2.0 Event Generation and Full one loop fermionic corrections, in preparation.
- [30] J. F. Gunion and H. Haber, hep-ph/9610337;  
M. Quiros, hep-ph/9609392.



**Fig. 1**

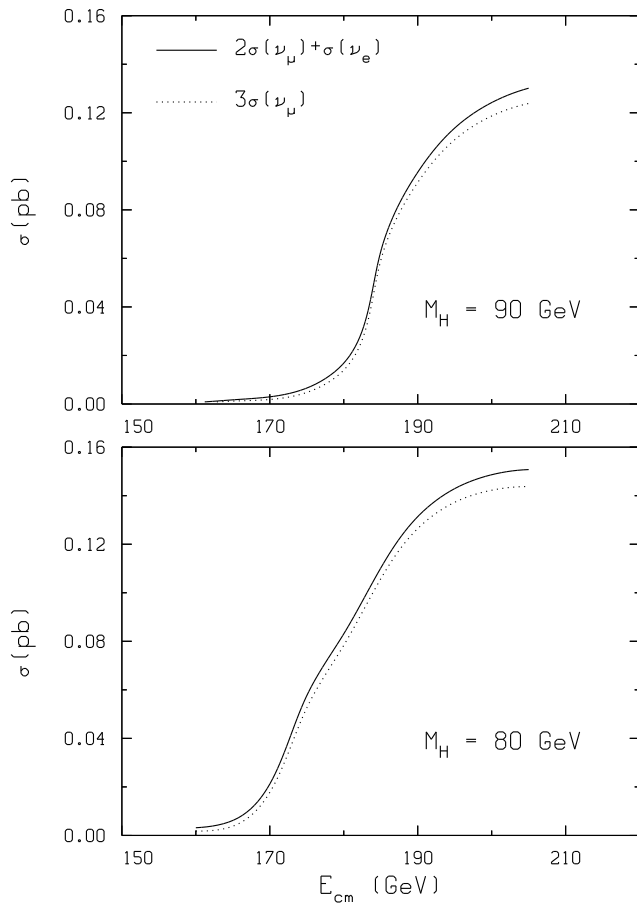


**Fig. 2**

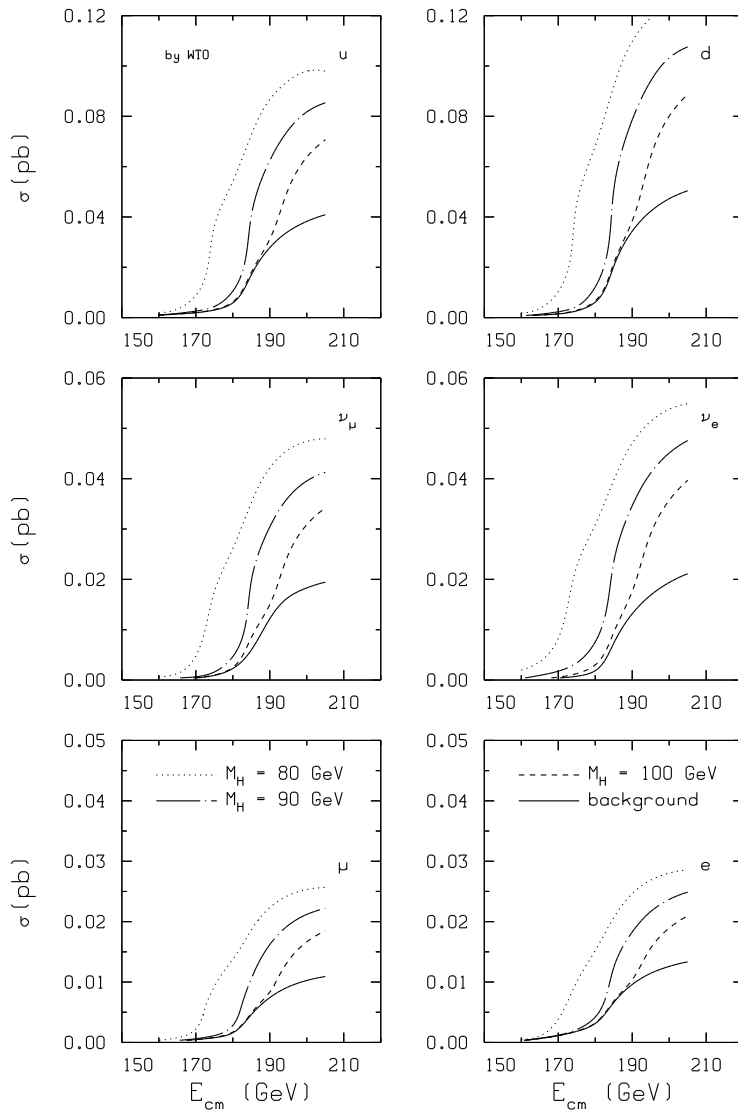


**Fig. 3**

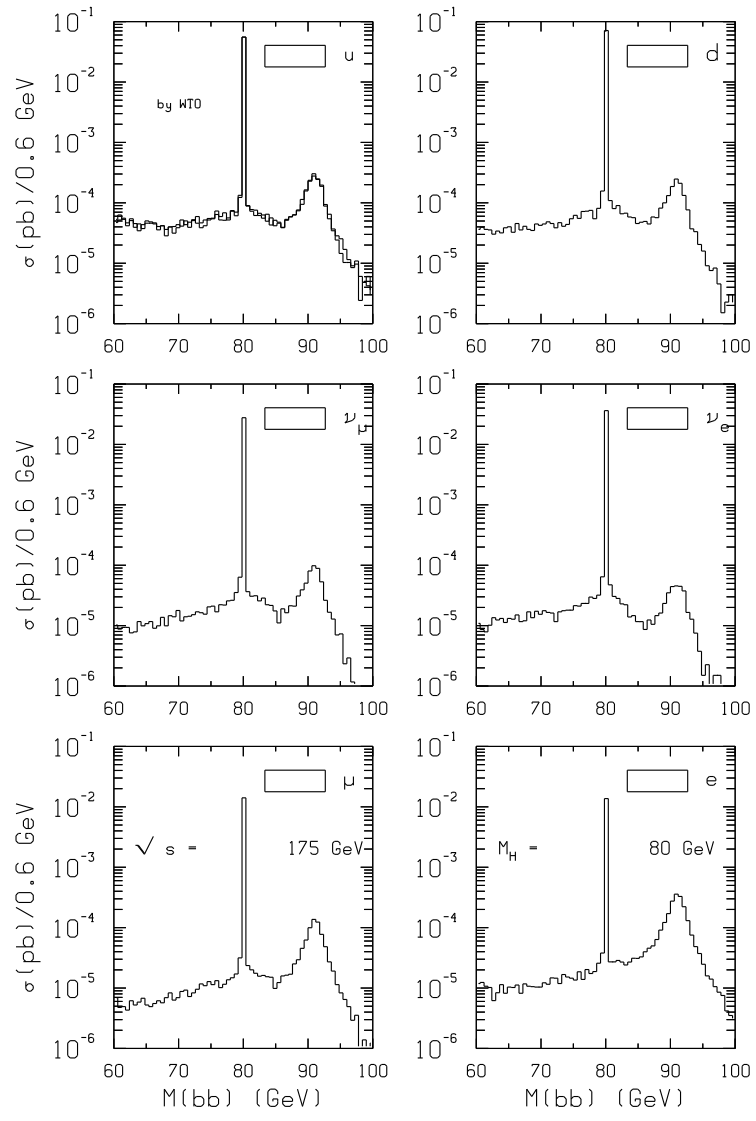


**Fig. 4**

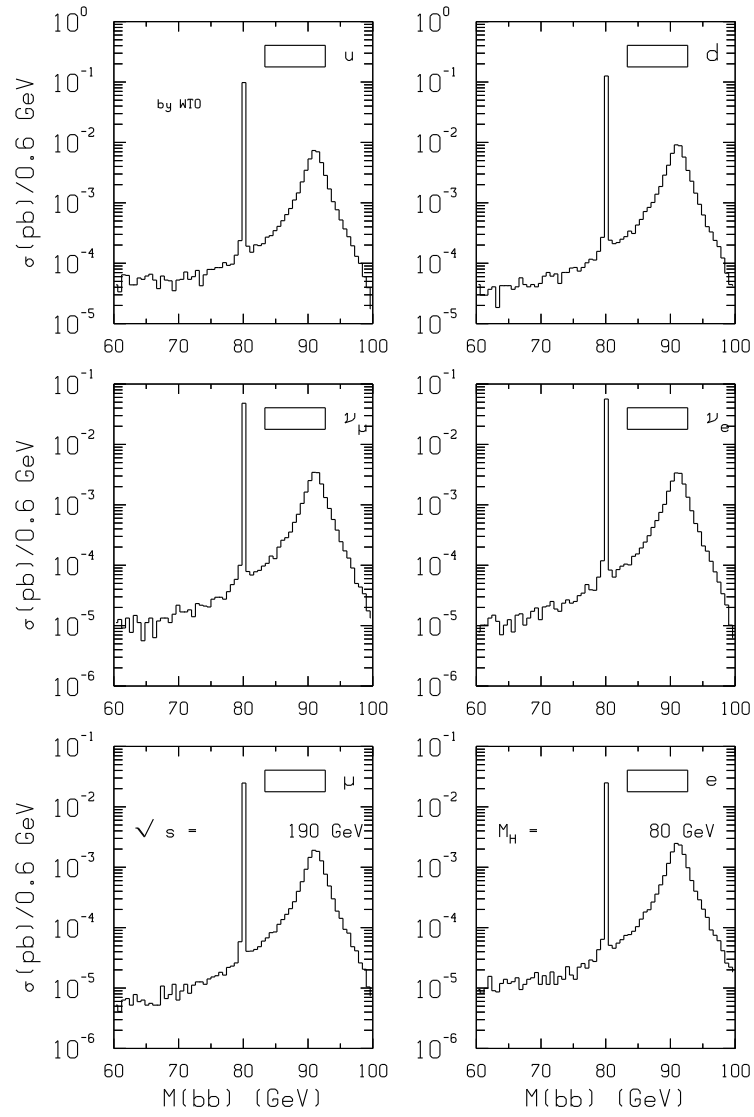


**Fig. 5**

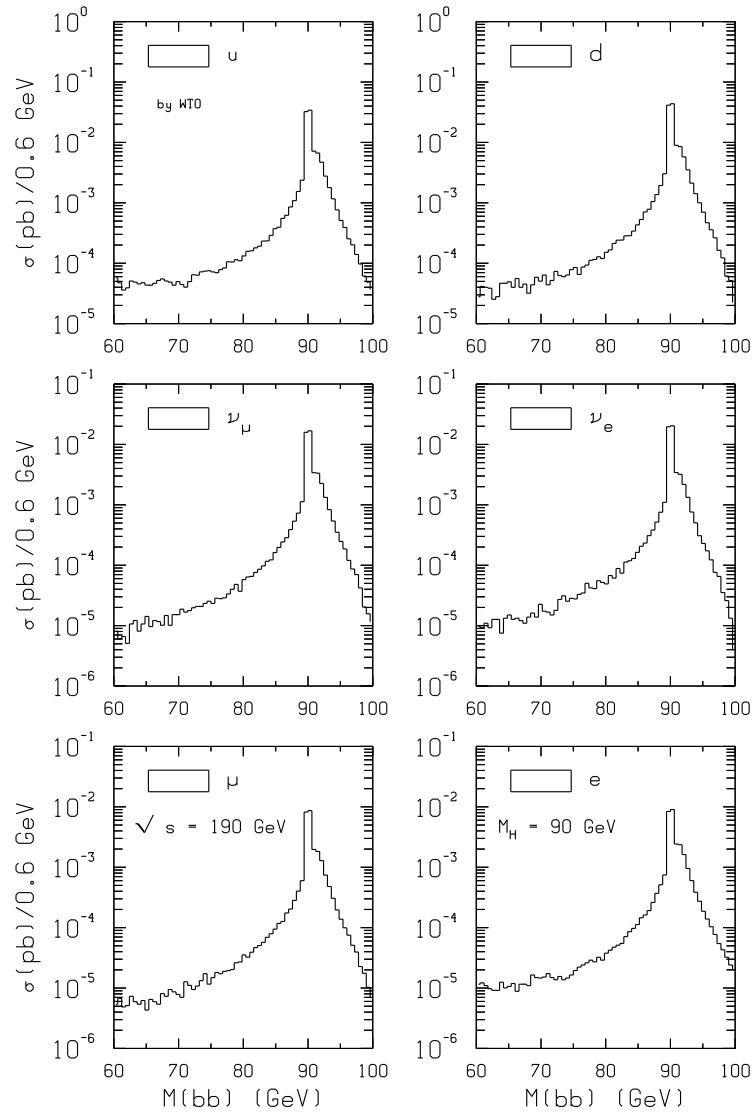


**Fig. 6**

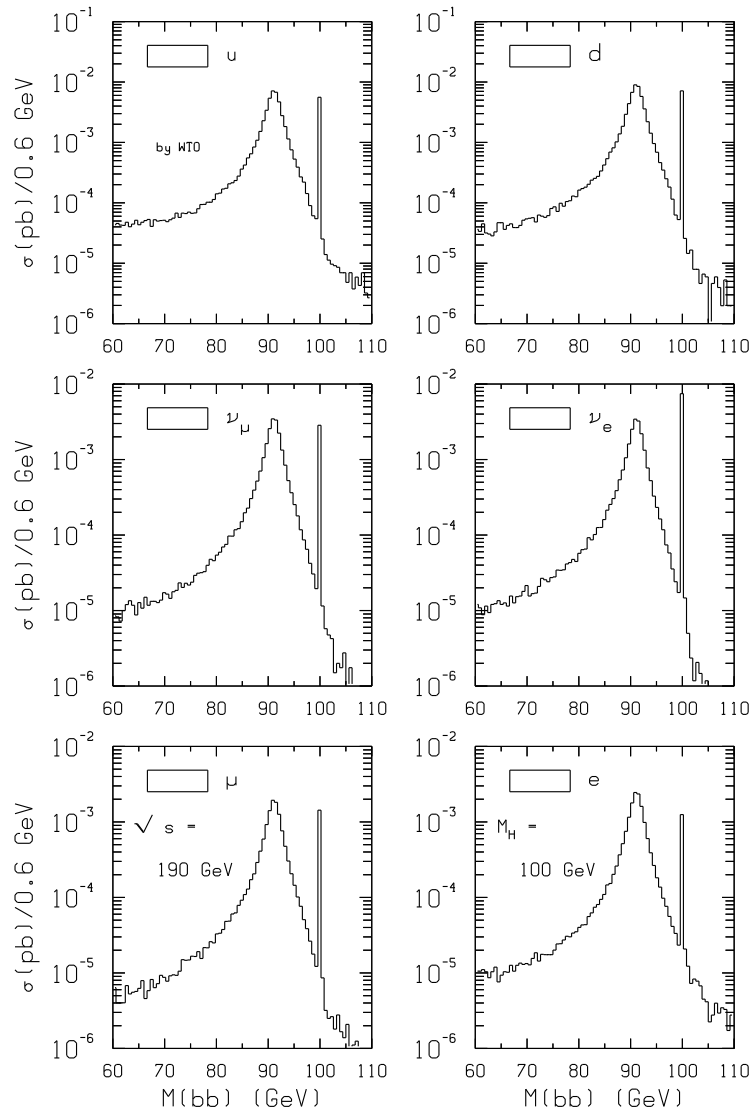


Fig. 7

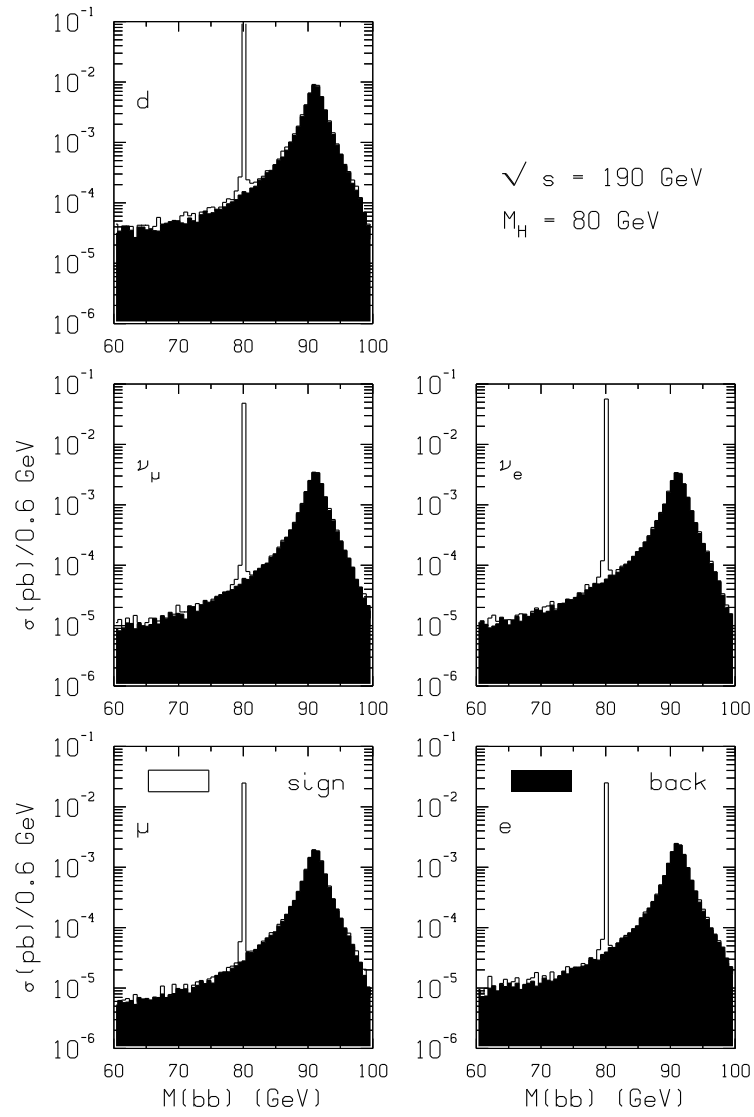


Fig. 8

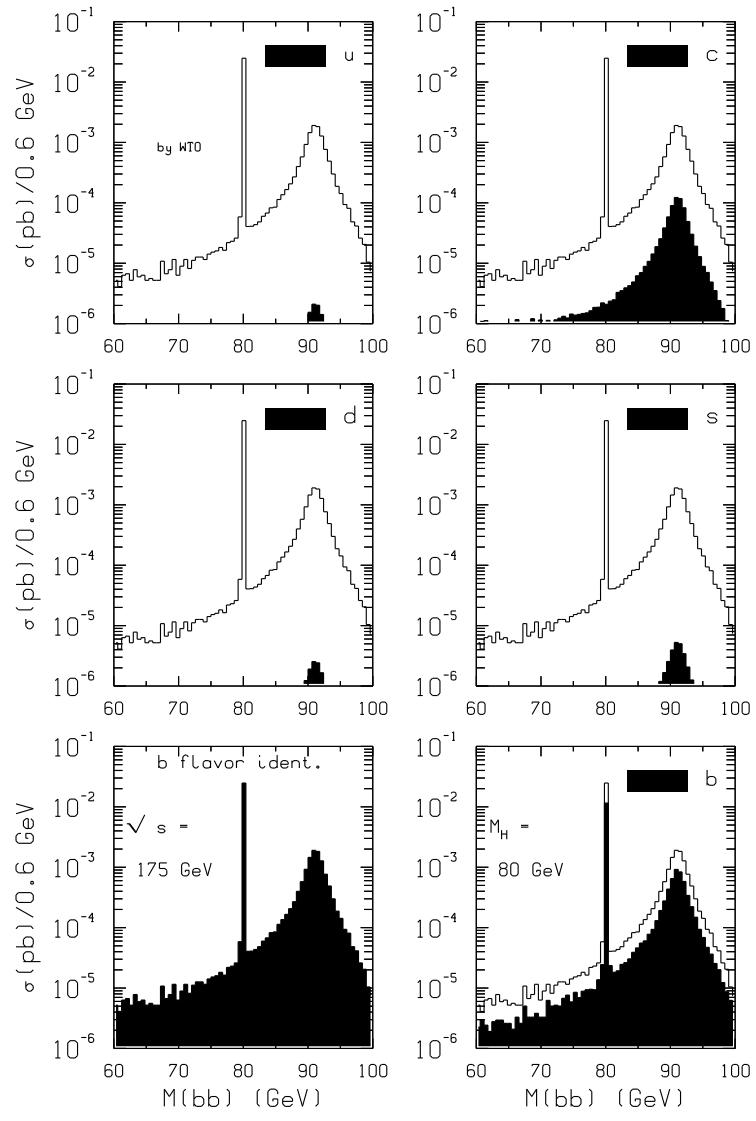


Fig. 9

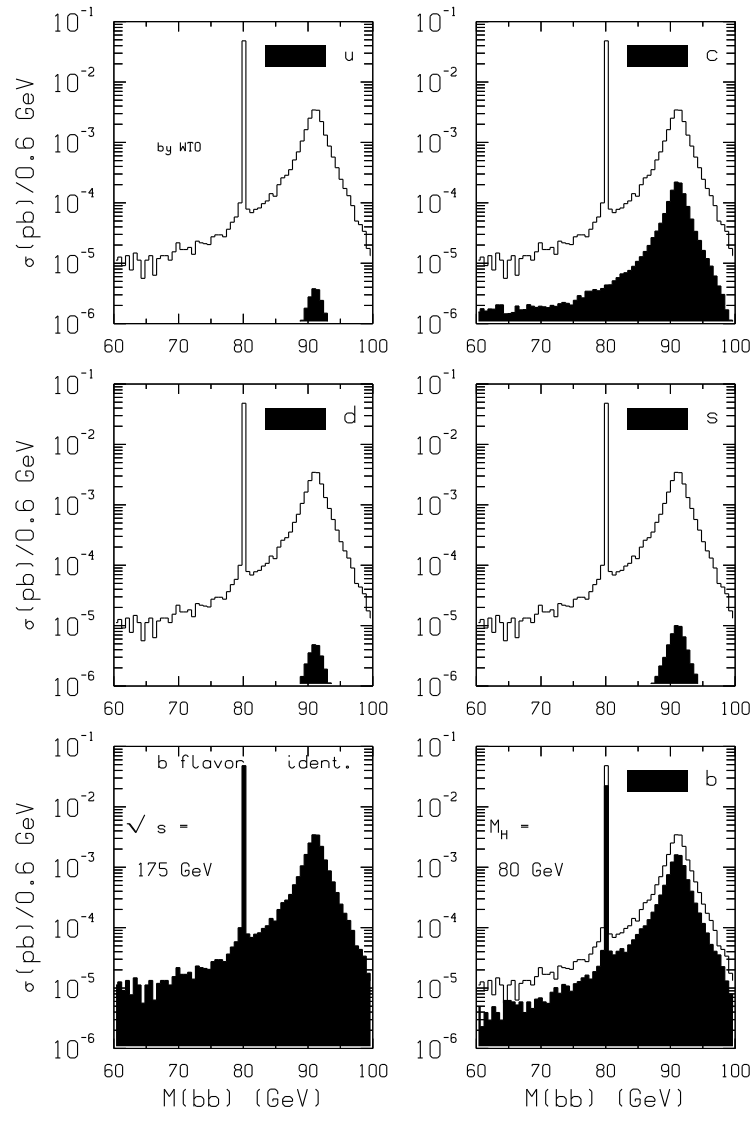


Fig. 10

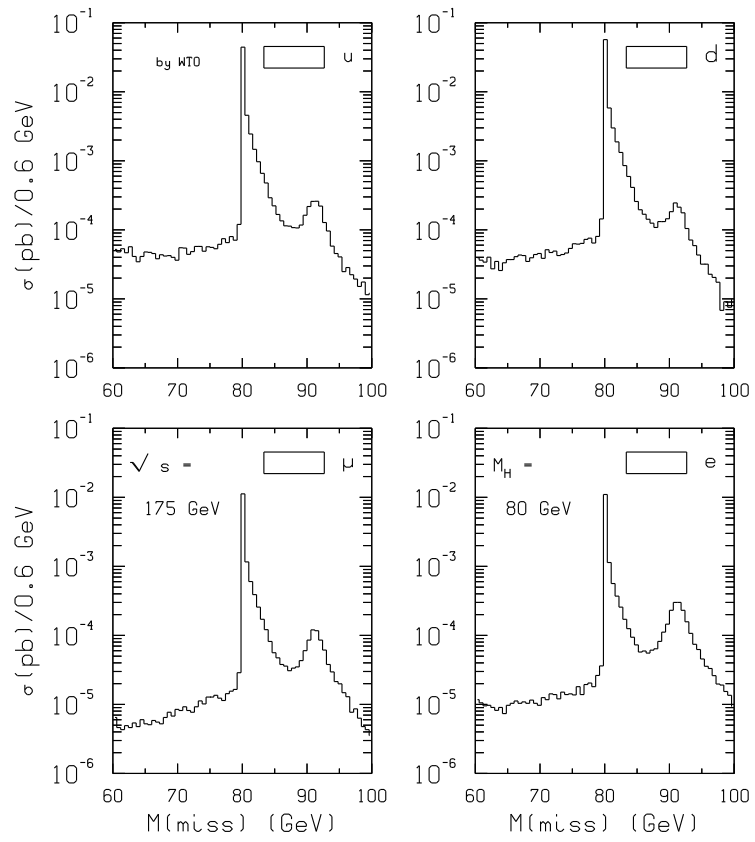


Fig. 11

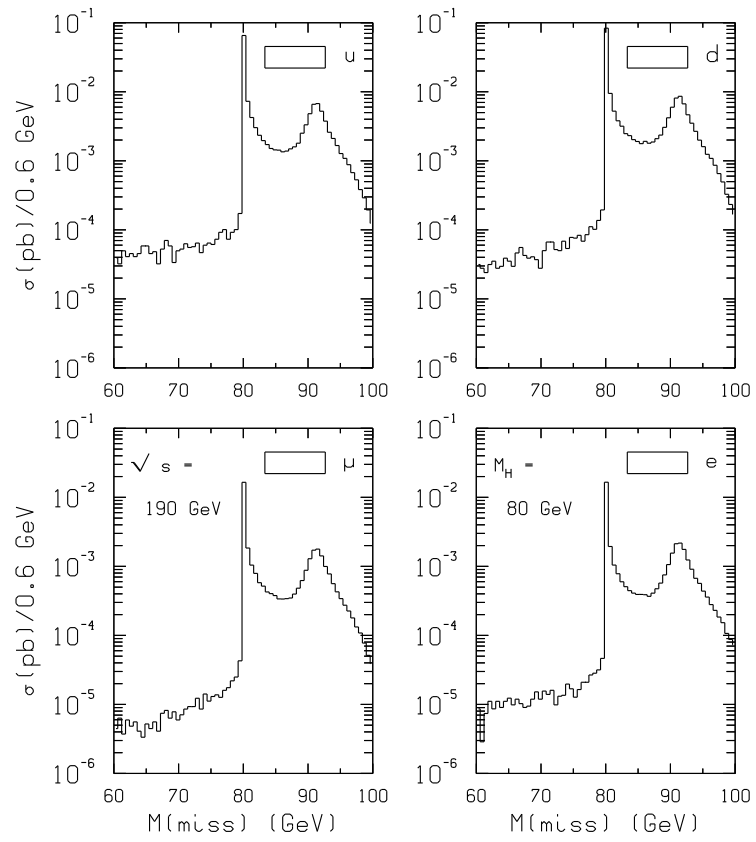
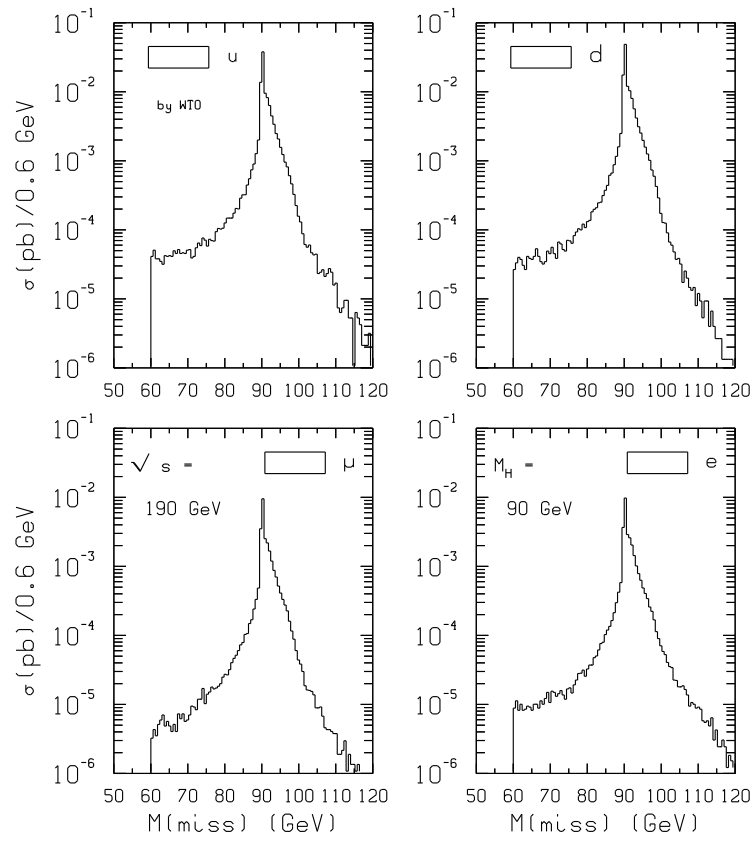
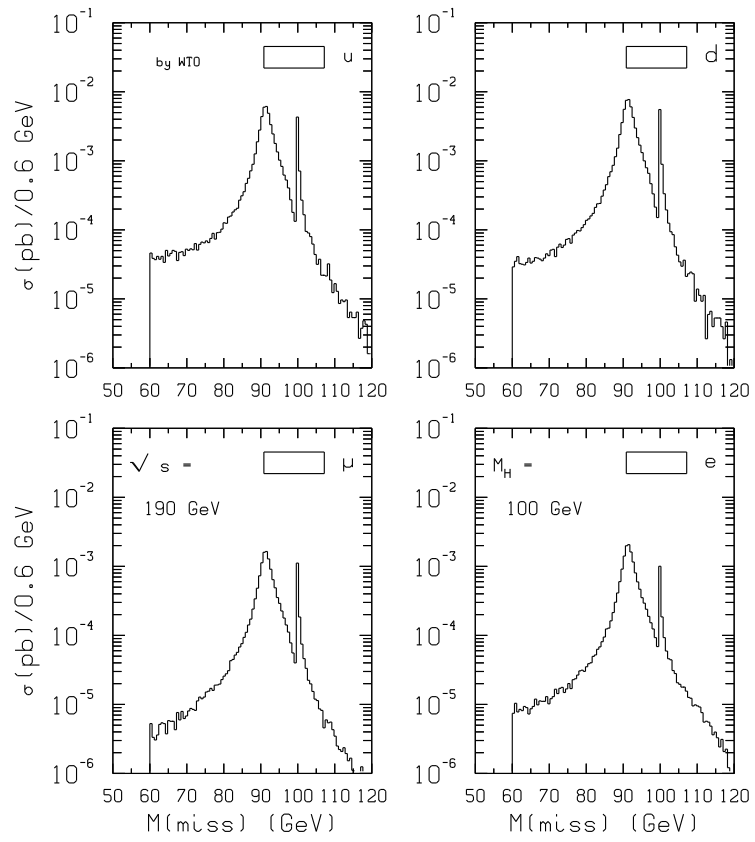


Fig. 12



**Fig. 13**



**Fig. 14**

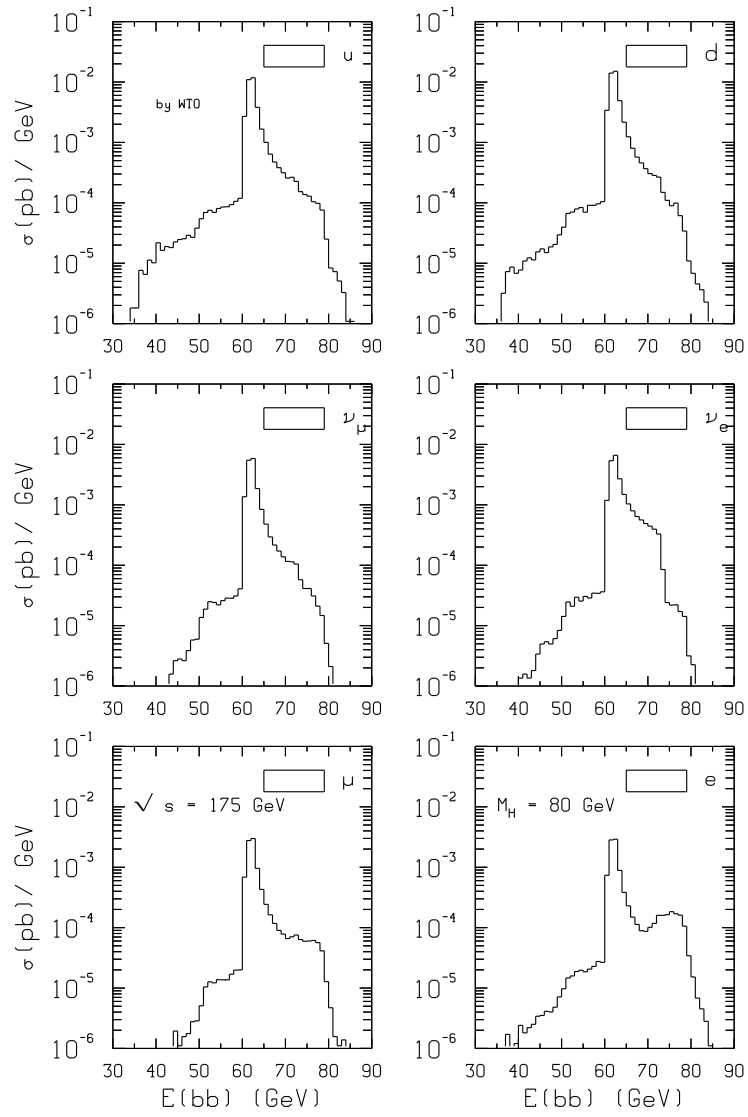


Fig. 15

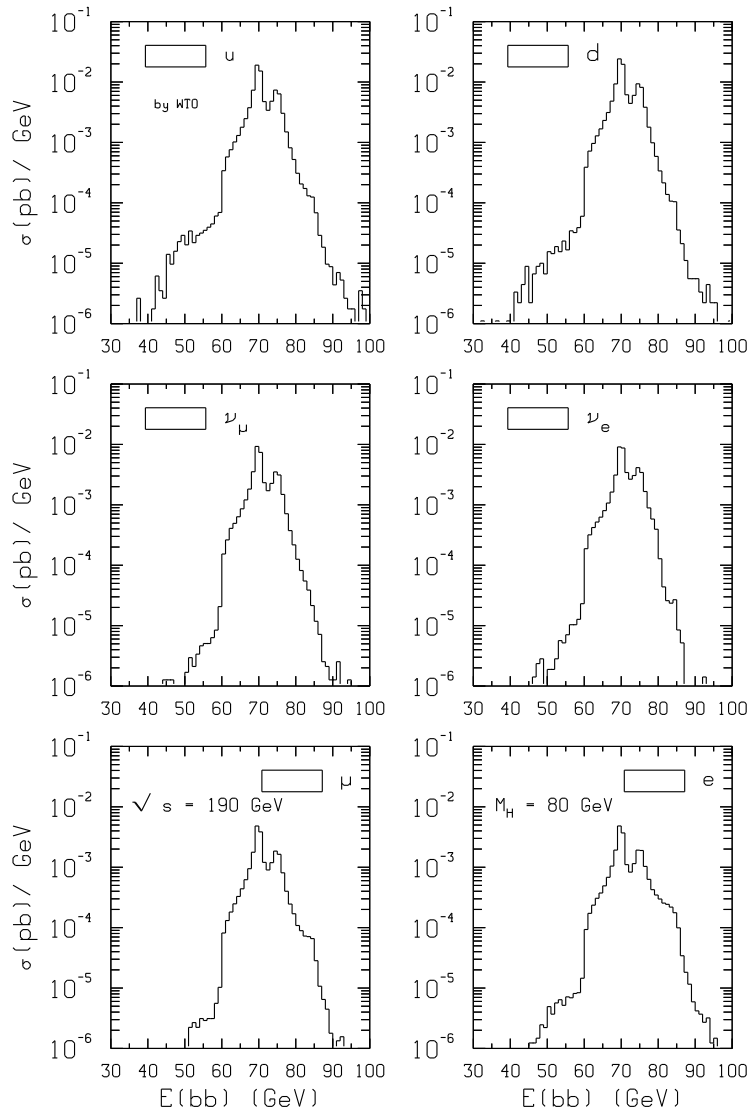


Fig. 16

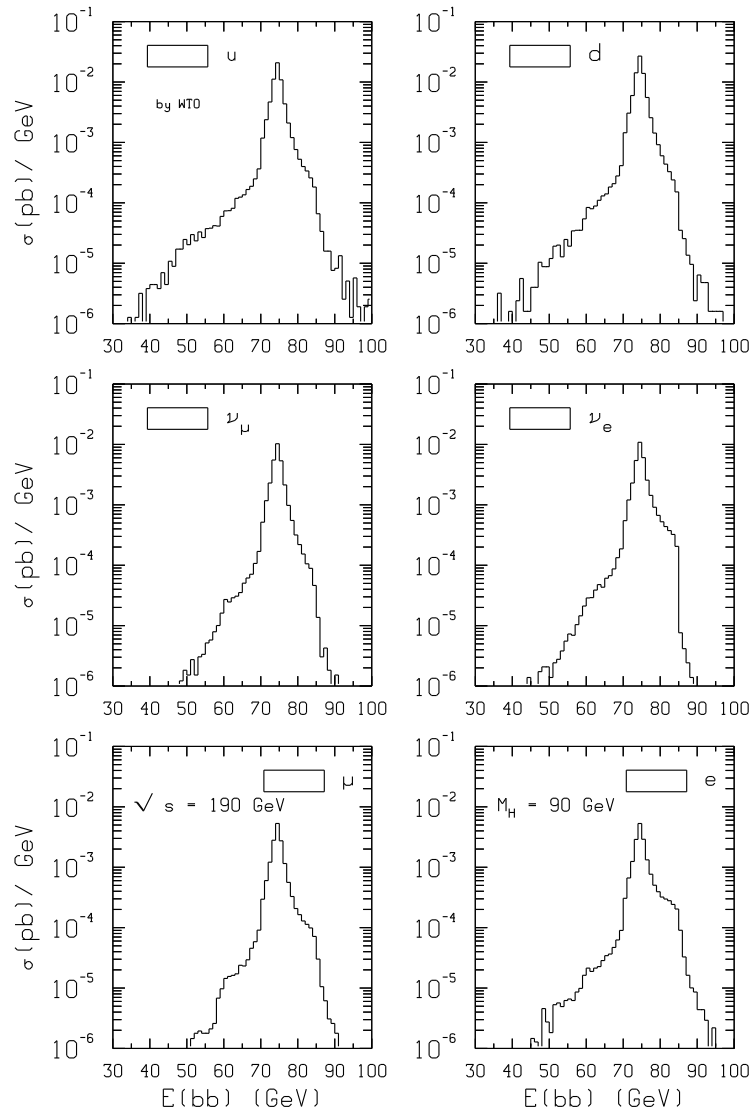


Fig. 17

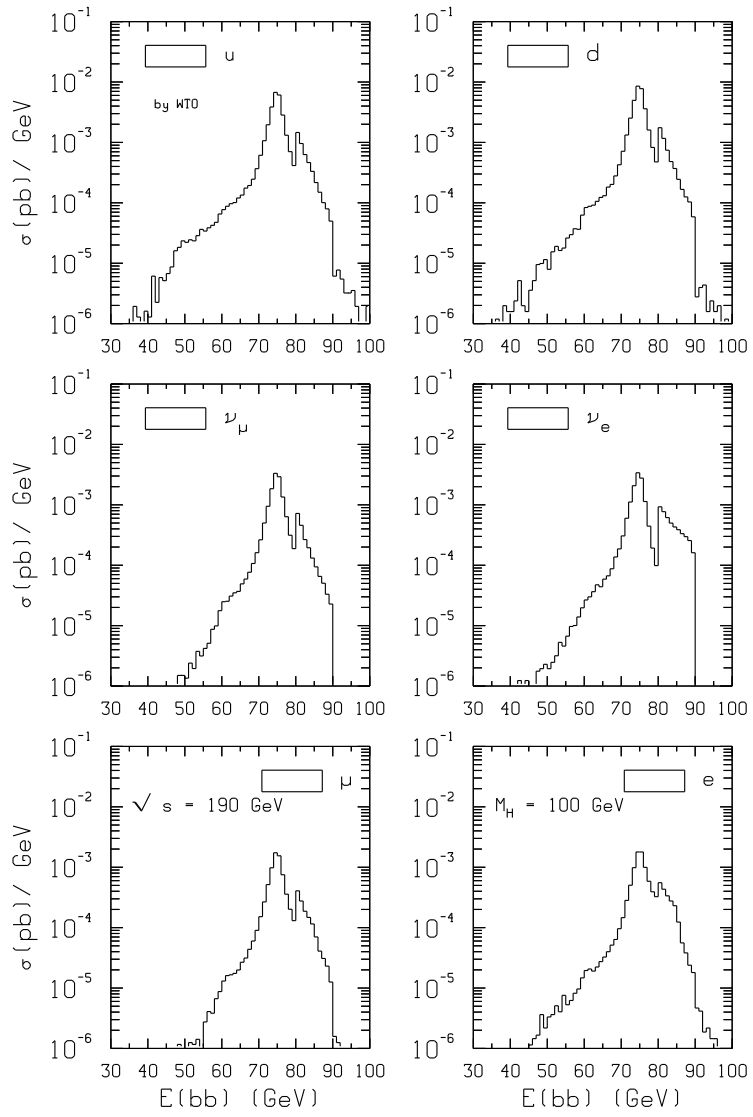
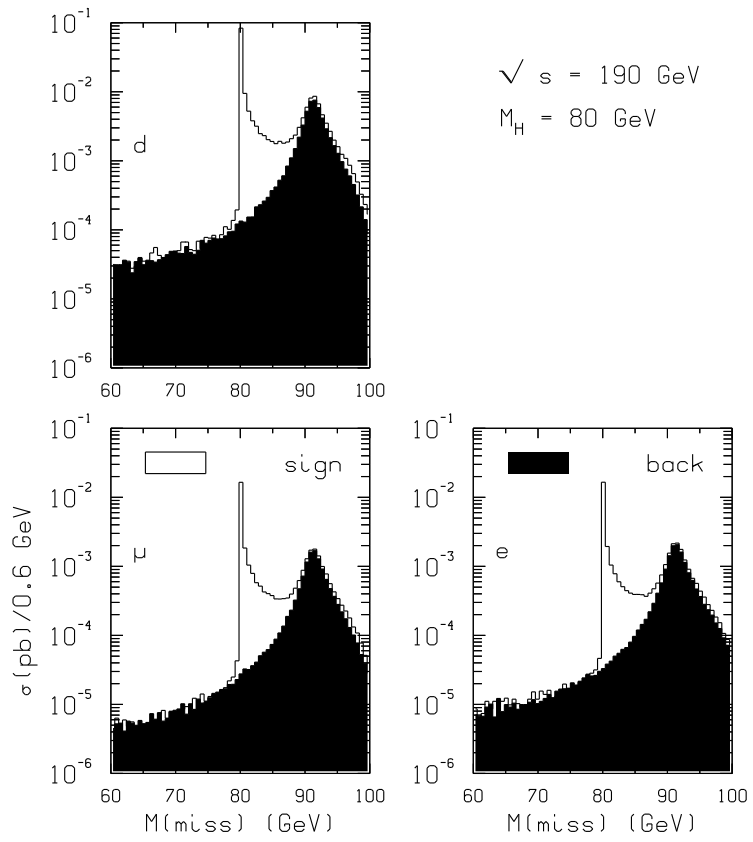


Fig. 18



**Fig. 19**

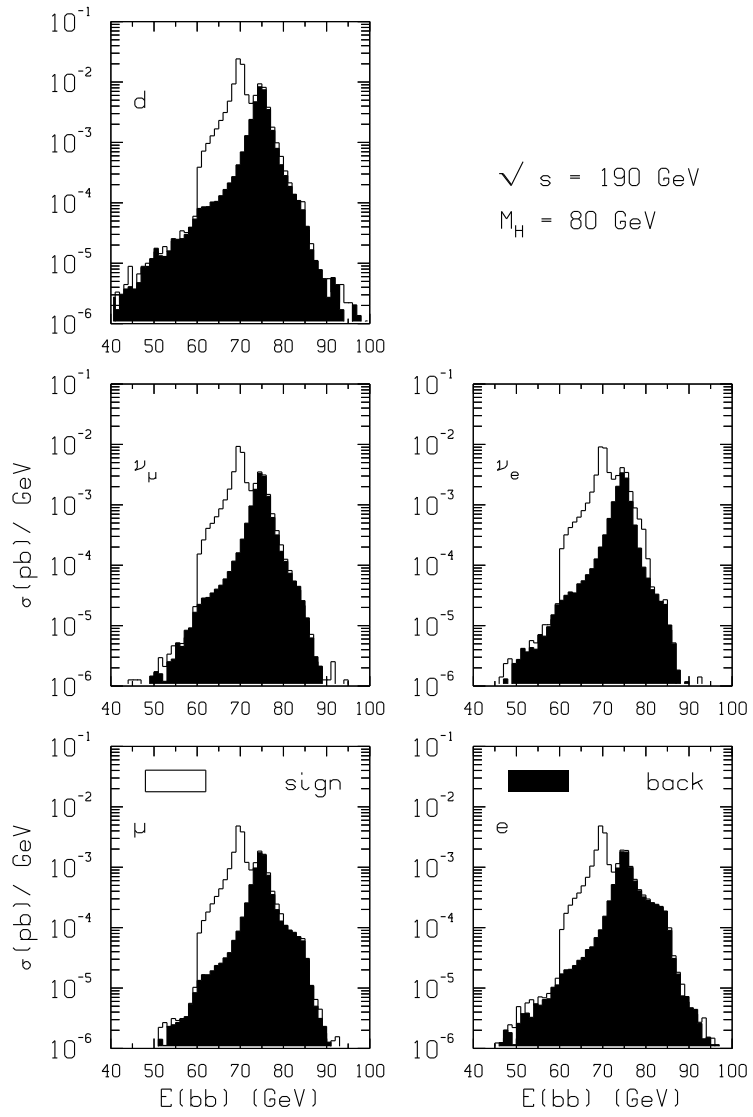


Fig. 20

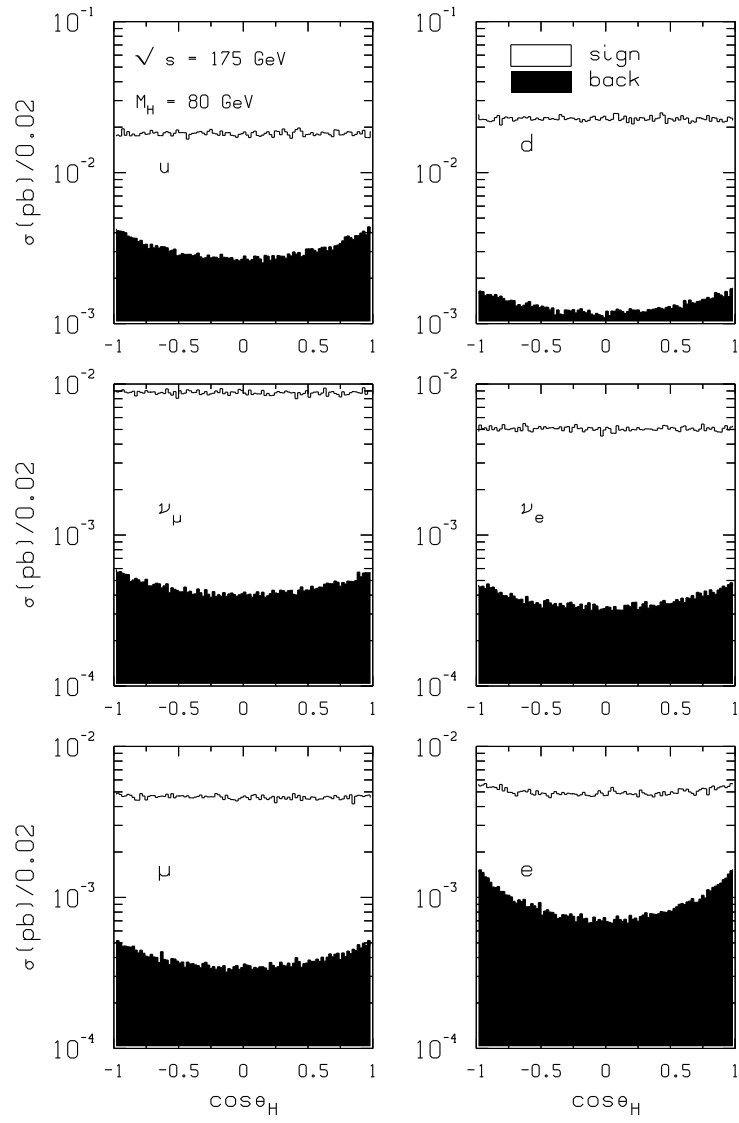


Fig. 21